Journal of Statistical Physics, Vol. 87, Nos. 3/4, 1997

Critical Phenomena with Convergent Series Expansions in a Finite Volume

Hildegard Meyer-Ortmanns[1] and Thomas Reisz[1,2]

Received April 17, 1996; final October 29, 1996

Linked cluster expansions are generalized from an infinite to a finite volume. They are performed to 20th order in the expansion parameter to approach the critical region from the symmetric phase. A new criterion is proposed to distinguish first- from second-order transitions within a finite-size scaling analysis. The criterion applies also to other methods for investigating the phase structure, such as Monte Carlo simulations. Our computational tools are illustrated with the example of scalar $O(N)$ models with four- and six-point couplings for $N=1$ and $N=4$ in three dimensions. It is shown how to localize the tricritical line in these models. We indicate some further applications of our methods to the electroweak transition as well as to models for superconductivity.

KEY WORDS: Finite-size scaling analysis; linked cluster expansions; scalar $O(N)$ models; critical phenomena; tricriticality.

1. INTRODUCTION

The phase structure of models for strong and electroweak interactions has been a topic of intensive research in the past. In spite of numerous investigations some central questions are still open. To these belong the nature of the chiral/deconfinement transition in QCD for physical values of the current quark masses and the strength of the electroweak transition for the physical (so far unknown) Higgs mass. In both realms one has to account for nonperturbative coupling regions. Thus it is natural to choose the lattice regularized version of these theories to study their phase structure. Most applications are performed with Monte Carlo simulations, which are an appropriate tool to study the critical region. Monte Carlo

[1] Institut für Theoretische Physik, Universität Heidelberg, D-69120 Heidelberg, Germany; e-mail: h.meyer-ortmanns@thphys.uni-heidelberg.de.

[2] Heisenberg fellow; e-mail: reisz@thphys.uni-heidelberg.de.

0022-4715/97/0500-0755$12.50/0

simulations are restricted to a finite volume. Thorough extrapolations to the infinite-volume limit from a finite-size scaling analysis are in general expensive and sometimes impracticable for lattice sizes which are realistic for QCD or for the standard model.[1]

Convergent expansions such as linked cluster, high-temperature, or hopping parameter expansions (HPEs) provide an analytic alternative to Monte Carlo simulations. They may also serve as a convenient supplement to numerical calculations. Originally they were developed in the *infinite* volume. In contrast to generic perturbation theory about noninteracting fields, HPEs are convergent power series expansions about completely disordered lattice systems. The expansion parameter κ is the coefficient of the (pair) interaction term. Under certain conditions their convergence radius can be directly related to the location of the physical singularity. Hence, similarly to Monte Carlo simulations, HPEs can be applied to the phase transition (critical) region if the order in the hopping parameter κ is just high enough. Thus the transition region is accessible from the high-temperature (symmetric) phase.

Hopping parameter expansions have a long tradition in statistical physics (see refs. 2–4 and references therein). Their generalization and application to particle physics were pioneered by Lüscher and Weisz,[5] who studied a lattice Φ^4-theory close to its continuum limit in four dimensions.[6,7] They were the first to perform such expansions by convenient algorithms with the aid of computers. In this way they succeeded to increase the highest available order in κ to 14 and generalized previous work to *arbitrary* values of the bare quartic coupling.

Recently, the HPE has been generalized to field theories at finite temperature.[8] The generalization is twofold. First, one has to implement a toroidal symmetry in one direction of finite extension, say L_0. In this context the temperature T is given by $T=L_0^{-1}$ in lattice units. Second, the highest computed order in the expansion parameter has to be increased, because the toroidal (temperature) effect on the critical coupling is rather small. Typically, the critical hopping parameter κ_c changes only by a few percent even on a $4\times\infty^3$ lattice compared to the ∞^4 lattice. The graphs of the expansion can only "feel the temperature" if they are able to wind around the torus in the temperature direction. In general, the largest possible winding number should be larger than one to induce a measurable effect. In ref. 9 the 18th order has been used to determine the critical behavior of the finite-temperature Φ^4 models with $O(N)$ symmetry. Meanwhile, the 20th order of this expansion is available for two-point susceptibilitites, see below.

In this paper we extend the HPE to a finite volume, i.e., to a lattice with toroidal symmetry in all directions. We propose criteria to distinguish

first- from second-order transitions (and crossover phenomena) both in an infinite and in a finite volume. It is the fate of power series expansions that one cannot work *at* the singularity κ_c, one can only come close to it—the closer, the higher the order in the expansion. Thus we need a criterion that works slightly below κ_c. As such a criterion we propose a so-called monotony criterion which is based on the specific volume dependence of truncated correlation functions close to, but not at the transition point. The criterion includes both order parameter susceptibilities and other singular response functions such as the specific heat. Decrease or increase with the volume identifies first- or second-order transitions, respectively. Although the monotony criterion has been developed in the framework of HPEs, it is not restricted to this case. It can be used in other methods as well, in particular in Monte Carlo simulations.

As a second application of the HPE in a finite volume we calculate an effective potential up to 16th order in the hopping parameter. The shape of the effective potential further characterizes the type of transition. The coexistence of distinct minima at the critical point provides another possibility to calculate κ_c in a finite volume.

The criteria will be applied to scalar $O(N)$ models with Φ^4 and Φ^6 self-interactions in three dimensions. These models allow for various first- and second-order transition regions in the bare coupling constant space. For fixed couplings the phase transitions will be considered as a function of κ. The parameter κ may be identified with an inverse temperature $1/T$ of a classical system with the same action in three dimensions. Thus in our applications HPEs are high-temperature expansions; sometimes we will replace κ_c by T_c^{-1}. Since the HPEs are performed for the free energy and connected correlations, they are linked cluster expansions. In connection with a field theory in four spacetime dimensions the three-dimensional model may be considered as an effective description of the four-dimensional model at finite temperature, arising in a process of dimensional reduction. In a four-dimensional theory at finite temperature one should distinguish between κ and T^{-1}.

The scalar $O(N)$ models contain a number of interesting special cases. If the four- and six-point couplings are sent to infinity in an approriate way, we obtain $O(N)$ models with random site dilution, i.e., Heisenberg models with additional occupation number variables, associated with the lattice sites; for $N=1$ we have a diluted Ising model (cf., e.g., ref. 14). The case of $N=4$ and pure quartic self-interaction is assumed to share the universality class with QCD in the limit of two massless flavors. It also corresponds to the scalar sector of the electroweak standard model. A $\Phi^4+\Phi^6$-theory exhibits a tricritical point (line) for a fixed (varying) six-point coupling. Such a tricritical point is observed in a liquid mixture of

^{3}He/^{4}He. Recently it has been also proposed as candidate for representing the universality class of *tricritical QCD*[10, 11] (tricritical QCD means QCD with vanishing up and down quark masses and a strange quark mass which takes a critical value, at which the chiral transition changes its order). We indicate how to localize the tricritical line in a $\Phi^4 + \Phi^6$-theory with our methods.

The outline of the paper is as follows. In Section 2.1 we summarize the main results for HPEs from ref. 8. It basically serves to fix the notation. We then extend the HPE in an infinite volume to a graphical expansion in a *finite* volume (Section 2.2). In Section 3 we give two criteria to distinguish first- from second-order transitions: a precise formulation of the *monotony criterion* (Section 3.1), and an effective potential evaluated in the HPE in a finite volume (Section 3.2). In Section 4 we apply these criteria to three-dimensional scalar $O(N)$ models with renormalizable interactions. To get a first estimate on the phase structure in bare coupling parameter space, we study the large-coupling limit by a saddle-point integration. Often this limit is the only coupling range of scalar $O(N)$ models that is studied in the literature. An estimate for the location at finite couplings is obtained from a hopping-mean-field analysis. This approximation amounts to a tree-level evaluation of the HPE (Section 4.1). After this preliminary study of the phase structure we present a more detailed investigation by means of the HPE for arbitrary finite couplings. In the infinite-volume limit, plateaus of critical exponents as obtained from the linked cluster series are proposed as criteria to identify the various universality classes of the critical region of the theory (Section 4.2). In Section 4.3 we discuss the finite-volume behavior of various quantities. The shift in volume of the critical coupling κ_c, defined here as the radius of convergence, is compared to the scaling behavior which is expected for the shift of the maximum of the order parameter susceptibility. The monotony criterion and the effective potential are evaluated for points both in the first- and second-order coupling region. Finally we show how to locate the tricritical line. In Section 5 we summarize our results and give the outlook for further physical applications.

The main emphasis of the paper lies in an explanation of the method rather than a list of results obtained in special cases of $O(N)$ models.

2. HOPPING PARAMETER EXPANSIONS FOR THE CRITICAL REGION

2.1. General Framework

Linked cluster expansions provide a convenient tool for both numerical and analytic studies of lattice field theories; The typical expansion

parameters are the coupling strengths between fields at different lattice sites.[2, 3] In contrast to saddle-point expansions, which are at most asymptotically convergent, series resulting from HPE are absolutely convergent for sufficiently small couplings.[12, 13] In this sense they can be viewed as generalized high-temperature expansions. If in addition the sign of the susceptibility series is uniform, the radius of convergence identifies the phase transition, i.e., the critical temperature.

In order to extract quantitative information on the critical behavior one has to get sufficiently close to the critical point. The price to be paid is a computation to high orders. The realization of such expansions by convenient algorithms with the aid of computers has been pioneered by Lüscher and Weisz.[5] Recently, progress in various ways has been made to extend the length of strong-coupling series.[8, 15, 16] Normally, these expansions are set up in an infinite volume. In ref. 8 the techniques have been further developed in such a way that the expansions can be reliably applied to lattices of nontrivial topology. In particular, it turned out that the highest order in the expansion had to be further increased for measuring effects from topology. The improved techniques have been applied to scalar $O(N)$ models with quartic interaction on four-dimensional finite-temperature lattices.[9] The critical exponents could be shown to agree with the critical indices of the corresponding (dimensionally reduced) three-dimensional models.

In the following we summarize the main formulas from refs. 5 and 8 to fix the notation and to set up the expansion scheme that later will be generalized to a finite volume. We consider a D-dimensional hypercubic lattice $\Lambda = \mathsf{X}_{i=0}^{D-1} \mathbb{Z}/L_i$, with $L_i \in \mathbb{N}$ an even number or with $L_i = \infty$. Periodic boundary conditions are imposed for each finite L_i. The restriction to even L_i leads to a considerable reduction of the number of contributing graphs because it implies that each loop must have an even number of lines. The class of models we discuss are described by the partition function

$$Z(J, v) = \int \prod_{x \in \Lambda} d^N \Phi(x) \exp\left[\tfrac{1}{2} \sum_{x \neq y \in \Lambda} \sum_{a,b=1}^{N} \Phi_a(x)\, v_{ab}(x, y)\, \Phi_b(y) \right]$$

$$\cdot \times \exp\left[- \sum_x \mathring{S}(\Phi(x)) + \sum_{x \in \Lambda} \sum_{a=1}^{N} J_a(x)\, \Phi_a(x) \right] \tag{1}$$

where Φ denotes a real, N-component scalar field, J are external sources, and $v_{ab}(x, y)$ denote the hopping couplings. The ultralocal part of the action $\mathring{S}$, which depends only on one lattice site, is chosen to be $O(N)$-invariant. It should guarantee the stability of the partition function (1) for

sufficiently small $v(x, y)$. Throughout this paper we consider as an example the action of a $\Phi^4 + \Phi^6$-theory

$$\mathring{S}(\Phi) = \Phi^2 + \lambda(\Phi^2 - 1)^2 + \sigma(\Phi^2 - 1)^3 \tag{2}$$

which exhibits a phase structure with both first- and second-order transitions. We emphasize, however, that the general techniques are not restricted to this case.

Fields at different lattice sites interact with the hopping coupling $v_{ab}(x, y)$. For the case of nearest neighbor interactions, it reduces to

$$v_{ab}(x, y) = \begin{cases} 2\kappa\delta_{a,b}, & x, y \text{ nearest neighbor} \\ 0, & \text{otherwise} \end{cases} \tag{3}$$

where κ is the so-called hopping parameter. The nearest neighbor property should be understood modulo the torus lengths. Henceforth we consider only nearest neighbor interactions.

The generating functional of connected correlation functions is given by

$$\begin{aligned} W(J, v) &= \ln Z(J, v) \\ W^{(2n)}_{a_1 \cdots a_{2n}}(x_1, \ldots, x_{2n}) &= \langle \Phi_{a_1}(x_1) \cdots \Phi_{a_{2n}}(x_{2n}) \rangle^c \\ &= \frac{\partial^{2n}}{\partial J_{a_1}(x_1) \cdots \partial J_{a_{2n}}(x_{2n})} W(J, v)\Big|_{J=0} \end{aligned} \tag{4}$$

In the following a major role is played by the connected two-point function and the corresponding susceptibility χ_2 and moments μ_2, defined according to

$$\begin{aligned} \delta_{a,b}\chi_2 &= \sum_x \langle \Phi_a(x)\, \Phi_b(0) \rangle^c \\ \delta_{a,b}\mu_2 &= \sum_x \left(\sum_{i=0}^{D-1} x_i^2 \right) \langle \Phi_a(x)\, \Phi_b(0) \rangle^c \end{aligned} \tag{5}$$

In field theory, it is convenient to define the renormalized coupling constants via the vertex functional

$$\begin{aligned} \Gamma(M) &= W(J) - \sum_{x \in \Lambda} J(x) \cdot M(x) \\ &= \sum_{n \geq 0} \frac{1}{(2n)!} \sum_{a_1, \ldots, a_{2n}} \Gamma^{(2n)}_{a_1 \cdots a_{2n}}(x_1, \ldots, x_{2n})\, M_{a_1}(x_1) \cdots M_{a_{2n}}(x_{2n}) \end{aligned} \tag{6}$$

$$M_a(x) = \frac{\partial W}{\partial J_a(x)}, \qquad a = 1, \ldots, n$$

The standard definitions of the renormalized mass m_R (as inverse correlation length) and the wave function renormalization constant Z_R are

$$\tilde{\Gamma}^{(2)}_{ab}(p, -p) = -\frac{1}{Z_R}(m_R^2 + p^2 + O(p^4))\,\delta_{a,b} \qquad \text{as} \quad p \to 0 \tag{7}$$

where the tilde denotes the Fourier transform. Equation (7) implies that

$$m_R^2 = 2D\frac{\chi_2}{\mu_2}, \qquad Z_R = 2D\frac{\chi_2^2}{\mu_2} \tag{8}$$

The critical exponents γ, ν, η are defined by the leading singular behavior at the critical point κ_c,

$$\begin{aligned} \ln \chi_2 &\simeq -\gamma \ln(\kappa_c - \kappa) \\ \ln m_R^2 &\simeq 2\nu \ln(\kappa_c - \kappa) \qquad \text{as} \quad \kappa \nearrow \kappa_c \\ \ln Z_R &\simeq \nu\eta \ln(\kappa_c - \kappa) \end{aligned} \tag{9}$$

such that $\nu\eta = 2\nu - \gamma$.

If the interaction part (3) of the action is switched off, i.e., $v = 0$, $S(\Phi, v = 0) = \sum_x \mathring{S}(\Phi(x))$, the partition function factorizes, and in turn $W(J, v = 0) = \sum_x \mathring{W}(J(x))$. In particular,

$$W^{(2n)}_{a_1 \cdots a_{2n}}(x_1, \ldots, x_{2n}) = \begin{cases} \dfrac{\mathring{v}^c_{2n}}{(2n-1)!!}\, C_{2n}(a_1, \ldots, a_{2n}) & \text{for } x_1 = x_2 = \cdots = x_{2n} \\ 0 & \text{otherwise} \end{cases} \tag{10}$$

with

$$\mathring{v}^c_{2n} = \frac{\partial^{2n}}{\partial J_1^{2n}} \mathring{W}(J)\bigg|_{J=0} \tag{11}$$

and C_{2n} totally symmetric coefficients in a_i, $i = 1, \ldots, 2n$.

In practice, the vertex couplings $\mathring{v}^c_{2n}$ are obtained from the relation

$$\begin{aligned} \mathring{W}(J) &= \sum_{n \geqslant 1} \frac{1}{(2n)!}\, \mathring{v}^c_{2n} (J^2)^n \\ &= \ln\left[1 + \sum_{n \geqslant 1} \frac{1}{(2n)!}\, \mathring{v}_{2n} (J^2)^n\right] \end{aligned} \tag{12}$$

with

$$\mathring{v}_{2n} = \frac{\int d^N\Phi\, \Phi_1^{2n} \exp(-\mathring{S}(\Phi))}{\int d^N\Phi \exp(-\mathring{S}(\Phi))} \tag{13}$$

or, alternatively, recursively from the Dyson–Schwinger equations.

The linked cluster expansion for W is the Taylor expansion with respect to $v(x, y)$ about this decoupled case,

$$W(J, v) = \left(\exp \sum_{x,y} \sum_{a,b} v_{ab}(x, y) \frac{\partial}{\partial \hat{v}_{ab}(x, y)} \right) W(J, \hat{v}) \Big|_{\hat{v}=0} \tag{14}$$

The corresponding expansions of correlation functions are obtained from (14) by (4). Susceptibilities become power series in κ with a nonvanishing radius of convergence.

The management of such an expansion is conveniently done by means of a graph-theoretic device. Correlation functions are represented as a sum over equivalence classes of graphs, each class being endowed with an appropriate weight. In order to make high orders in the expansion feasible it is necessary to introduce more restricted subclasses of graphs such as one-particle irreducible (1PI) graphs, one-vertex irreducible graphs, and renormalized moments. The correlations are then represented in terms of the latter two. For further details we refer to refs. 5 and 8.

The total weight of each graph consists of a rational weight factor decomposing into a product of its (inverse) symmetry number, the $O(N)$-group factor, and the lattice embedding number, and a product of $\mathring{v}^c_{2n}$'s of Eq. (11). It is only the lattice embedding factor that depends on the topology of the particular lattice which is involved. In the next section we outline the modifications of the embedding numbers due to a finite volume. Explicit examples of series for χ_2 are given in Appendix B.

2.2. Extension to the Torus

Let us consider a correlation function, such as in (5), on a D-dimensional lattice of size $L_0 \times L_1 \times \cdots \times L_{D-1}$ with periodic boundary conditions. Except for a trivial volume factor, the embedding number $I_\Gamma(L_0, \ldots, L_{D-1})$ of a connected graph Γ counts the number of possible ways Γ can be embedded on the lattice. Embedding means a mapping of every vertex v of Γ onto a lattice site $x(v) = (x_0, \ldots, x_{D-1})(v)$ consistent with the topology of Γ. Every two vertices have to be mapped to nearest neighbor lattice sites if they are neighbored vertices of Γ, i.e., if they are connected by at least one line. Self-lines do not exist. Otherwise the linked

cluster expansion does not impose any exclusion constraints. In particular, an arbitrary number of vertices can occupy the same lattice site. This kind of lattice embedding is sometimes called a "free embedding."

It is most convenient to rearrange the computation of embedding numbers in terms of random walks.[5] Toward this end, the set of vertices of Γ is divided into the disjoint sets of internal 2-vertices and their complement. A vertex v is called an internal 2-vertex if it has no external line attached and there are precisely two neighbored vertices of v in Γ. All internal 2-vertices can be reorganized into so-called 2-chains between the remaining vertices in an obvious way. Every 2-chain c has an initial vertex i_c and a final vertex f_c, possibly identical, and it has a length $l_c \geqslant 1$, where $l_c - 1$ denotes the number of internal 2-vertices of c. Here, for convenience, we include $l_c = 1$, in which case c just implies the nearest neighbor constraint on i_c and f_c. On the lattice infinite in all directions the embedding number is then written as

$$I_\Gamma(\infty^D) = \sum_{(x(v))}{}' \prod_c \mathcal{N}^{l_c, D}_{x(i_c) \to x(f_c)}(\infty^D) \tag{15}$$

The sum runs over all placements of vertices v that are not internal 2-vertices, with $x(v_0)$ kept fixed for some arbitrary vertex v_0 to account for the trivial entropy factor. The product runs over all 2-chains of Γ. Here $\mathcal{N}^{l, D}_{x \to y}(\infty^D)$ denotes the number of free random walks of length l from lattice site x to y. Closed analytic expressions can be given for $\mathcal{N}^{l, D}_{x \to y}$. We notice that

$$\mathcal{N}^{l, D}_{x \to y}(\infty^D) \neq 0 \qquad \text{only if} \quad l - \sum_{i=0}^{D-1} |x_i - y_i| \geqslant 0 \quad \text{even} \tag{16}$$

In the finite volume with periodic boundary conditions the topology modifies (15) at two places. First, the sites $x(v)$ are now restricted to a cube of size $L_0 \times L_1 \times \cdots \times L_{D-1}$, and the nearest neighbor constraint, implicit in every 2-chain c of length $l_c = 1$, holds modulo the torus lengths. Second, the number of random walks $\mathcal{N}^{l_c, D}_{x \to y}(\infty^D)$ is replaced by

$$\mathcal{N}^{l_c, D}_{x \to y}(L_0, \ldots, L_{D-1}) = \sum_{\mu_0, \ldots, \mu_{D-1} \in \mathbb{Z}} \mathcal{N}^{l_c, D}_{x \to y + \mu \cdot L}(\infty^D) \tag{17}$$

where

$$\mu \cdot L = \sum_{i=0}^{D-1} \mu_i L_i$$

The sum in (17) accounts for additional random walks which arise from the possible winding around the torus. Due to (16), the sum in (17) is finite.

3. FINITE-SIZE SCALING ANALYSIS WITH HPE

In this section we discuss two criteria in the finite volume to determine the order of a phase transition. Although the criteria are developed for linked cluster expansions, their application is not restricted to series representations.

The question arises of why one is interested in linked cluster expansion on a torus, since the expansion is more easily obtained in the infinite volume. Data on the critical region such as the critical temperature are successfully extracted from the asymptotic high-order behavior of the coefficients of susceptibility series. The typical precision here is within 4–5 digits or even better.

In general the symmetry of the model alone does not determine the properties of a transition. For instance, there may be more than one universality class, corresponding to different ranges in the space of bare actions. As was pointed out in ref. 9, one should look for plateaus of critical exponents to distinguish between them. Problems arise close to the boundary of two such domains. "Smearing effects" occur due to the truncation of the series. Both universality domains will influence the coefficients—the more, the lower the order. This does not pose a problem, as long as the domains are sufficiently large and the boundary of the domains extends over a negligible coupling range.

Whereas the location of the phase transition can be determined very precisely from the infinite-volume series, its order is usually a more intricate question, in particular, if the transition is weakly first order. Criteria to distinguish first- and second-order transitions can be conveniently worked out in the finite volume. Thus, in our case, the finite-size effects will be utilized rather than suppressed as artifacts of the finite volume.

A finite-size scaling analysis for second-order transitions can be based on a renormalization group approach; see, e.g., ref. 17. The inverse linear size L^{-1} of the system is put on an equal footing with other scaling fields such as the temperature or an external field. The analysis results in a prediction of the leading scaling behavior of a susceptibility χ about the critical temperature T_c according to

$$\chi(t, L) \simeq |t|^{-\gamma} P(L/\xi_\infty(t)) \tag{18}$$

for sufficiently small t and large L, where t is the reduced temperature $(T-T_c)/T_c$ and γ is the critical exponent characterizing the divergence at $t=0$. The amplitude P depends only on L measured in units of the infinite-volume correlation length ξ_∞. Further properties of P ensure that at the temperature $T_c(L)$ where the susceptibility has its maximum the height of this peak scales according to $\chi(T_c(L), L) \simeq L^{(\gamma/\nu)}$, the width $\sigma(L)$ of the critical region shrinks with $L^{-1/\nu}$, and $T_c(L)$ is shifted compared to T_c according to $T_c(L)-T_c \simeq L^{-1/\nu}$. Here ν denotes the critical exponent of the correlation length.

For a generic first-order transition an analogous derivation of the scaling behavior from first principles is missing in general. The ratio $L/\xi_\infty(t)$ is no longer a distinguished scaling variable. In the thermodynamic limit, as T approaches T_c, the correlation stays finite and model dependent. The rounding and shifting of thermodynamic singularities are normally described in a phenomenological approach[18] which is based on Monte Carlo results. The height of the peak of the susceptibility at $T_c(L)$ is expected to scale with L^D, and both the width $\sigma(L)$ and the shift in $T_c(L)-T_c$ are expected to scale with L^{-D} as $L \to \infty$, where D denotes the space(time) dimension. A more fundamental finite-size scaling theory exists for a class of spin models that allow for a particular polymer expansion of the partition function.[19] Whereas the predictions of the finite-size scaling of the height of the peak and the width of the scaling region reproduce the above-mentioned behaviour, the shift of the location of the peak is derived to be $T_c(L)-T_c \simeq L^{-2D}$.

It turns out that our series representations in the hopping parameter κ for the susceptibilities χ cannot be uniquely extrapolated to the critical κ_c (corresponding to T_c^{-1} as explained in the introduction) to the end that the peak and width of χ confirm the expected scaling behavior. However, the specific behavior of χ close to κ_c is conclusive enough for distinguishing regions of first- and second-order transitions, as we will show below, without any need for an extrapolation in κ to κ_c. In addition, the scaling of $\kappa_c(L)$, defined as the radius of convergence in the finite volume, follows the form expected (by analogy) for the shift of the location of the peak from ref. 19. The scaling behavior holds for the $\mathbb{Z}_2$ model, but also for the $\Phi^4+\Phi^6$-models with four components, which are not covered by the analysis of ref. 19; cf. Section 4.3.

3.1. The Monotony Criterion

For a certain interval of the scaling region, response functions with a nonanalytic behavior in the infinite-volume limit show different monotony behavior for first- and second-order transitions. Examples of such functions

are the specific heat and order parameter susceptibilities. They are increasing in volume in a certain neighborhood of T_c for second-order transitions, and decreasing for first-order transitions for some range in the scaling region, which will be specified below. Since we are not aware of any discussion in the literature, although the underlying idea is rather simple, we will describe the behavior in some detail. For definiteness we fix the notation in terms of order parameter susceptibilities.

In the following it is convenient to write the susceptibilities as a function of L and $t \equiv t(L) \equiv T - T_c(L)$. Here $t(L)$ measures the temperature distance to the location of the maximum of $\chi(T, L)$ in volume L^D. From the standard finite-size scaling analysis one knows that in the infinite volume

$$\chi(t + T_c(L), L = \infty) < \infty \qquad \text{as} \quad t \to 0 \tag{19}$$

for a first-order transition with a possible discontinuity, whereas

$$\chi(t + T_c(L), L = \infty) \simeq \mathscr{A} |t|^{-\gamma} \tag{20}$$

for a second-order transition with critical exponent $\gamma > 0$. By definition, regular contributions to χ may be neglected in the scaling region. On the other hand, $\chi(T_c(L), L)$ diverges in both cases as L approaches infinity. More precisely, at $T_c(L)$, χ has a "δ-function" or power-law type of singularity for a first- or second-order transition in the thermodynamic limit, respectively. It is this difference that is responsible for the different monotony properties for $t \neq 0$ in the finite volume.

If $\delta \neq 0$ is small, to a given lattice size $L_s < \infty$, not too small (in order to satisfy the standard assumptions of the finite-size scaling analysis), one can always find a second size L_l with $L_l > L_s$ such that (cf. Fig. 1)

$$\chi(\delta + T_c(L), L \geqslant L_l) > \chi(\delta + T_c(L_s), L_s) \qquad \text{for} \quad \text{2nd order} \tag{21}$$

$$\chi(\delta + T_c(L), L \geqslant L_l) < \chi(\delta + T_c(L_s), L_s) \qquad \text{for} \quad \text{1st order} \tag{22}$$

that is, $\chi(\delta + T_c(L), L)$ is increasing or decreasing in volume. We notice that in (21) and (22) the susceptibilities are measured at fixed distance from their respective maxima. The range of δ where (21) and (22) are supposed to hold satisfies

$$c_1 \sigma(L)^{1/(1+\varepsilon)} < |\delta| < c_2 \sigma(L_s) \tag{23}$$

Here $\sigma(L)$ denotes the width of the critical region in the volume L^D, and c_1, c_2 and ε are positive constants, typically with $\varepsilon = 1$. Beyond the general constraint that both volumes L_s and L_l have to be sufficiently large, in

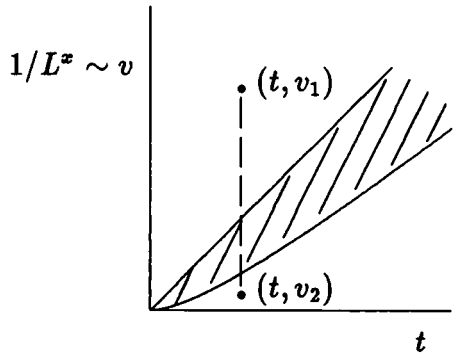

Fig. 1. The (t, v) plane for susceptibilities $\chi(t, v) > 0$ in the vicinity of a phase transition at $(t = 0, v = 0)$; t denotes the scaling field, $t = (T - T_c(L))/T_c(L)$, and v is the inverse of some power of the volume L^x with some $x > 0$. For a first-order transition, $\chi(t, v_1) > \chi(t, v_2)$, whereas for a second-order transition $\chi(t, v_1) < \chi(t, v_2)$. For the shaded part no prediction is made.

addition L_l has to be sufficiently larger than L_s, so that $\sigma(L_l)$ is considerably smaller than $\sigma(L_s)$. We would like to stress that the monotony behavior of χ does *not* refer to values of L_l close to L_s. In terms of Fig. 1, L_s and L_l are separated by the shaded area, for which we do not make any predictions.[3]

In the series representation of χ we can set $L_l = \infty$, so that (21) and (22) give strong criteria in the whole scaling region where we can use the series.

In the following we make these statements more precise, in order to show that the monotony behavior is neither a pecularity of specific models nor an artifact of the series expansion. It is a generic feature of models with first- and second-order transitons if the standard assumptions on their finite-size scaling behavior apply. Rigorous proofs of these assumptions are missing in general, neither do we attempt to give such proofs in the treatment below.

Let t denote the scaling field, i.e., $t = (T - T_c(L))/T_c(L)$. Here $T_c(L)$ locates the maximum of the susceptibility in the volume L^D. Furthermore, we set $v = L^{-m}$ with $m > 0$. The infinite-volume limit is obtained as $v \to 0$ from above. Equally well, we could have set $t = (T - T_c)/T_c$. If $T_c(L) - T_c$ shrinks at least as fast as the width of the critical region, as the standard assumptions on finite-size scaling analysis predict, the following statements would be left unchanged.

[3] Accordingly, the results of Esser *et al.*[34] do not contradict our lemmas. The nonmonotonic behavior of the susceptibility they found may be caused by a choice of L_s too small for the regular contributions to χ to be really negligible, or by a choice of L_l too close to L_s.

The transition range is given by small t and v. Let

$$H^2 := \{(t, v) \in \mathbf{R}^2 \mid v \geqslant 0\} \tag{24}$$

denote a half-plane, $\mathcal{U} \subseteq H^2$ the intersection of an open neighborhood of $0 \in \mathbf{R}^2$ with H^2, and $\mathcal{U}^* = \mathcal{U} \setminus \{0\}$.

We discuss the case of a first-order transition first. The typical behavior of a susceptibility close to the transition is described by the following definition.

Definition 3.1. For any $\omega > 0$ we define $\Psi_1^{(\omega)}(\mathcal{U})$ as the set of real-valued continuous functions $\chi: \mathcal{U}^* \to \mathbf{R}$ with the following properties.

1. $\chi \in C^1(\mathcal{U}^* \setminus \{(\mathbf{R}, 0)\})$, that is, χ is once continuously differentiable for $v \neq 0$.

2. For all nonzero t there is $\nu_t > 0$ such that for all $v < |t|/\nu_t$

$$|\chi(t, v)| \leqslant \omega$$

3. With appropriate positive constants c, K_1, K_2, and ε we have in $\mathcal{U}^*$ for $v \neq 0$

$$\left|\chi(0, v) - \frac{c}{v}\right| < \frac{K_1}{v^{1-\varepsilon}}$$

$$\left|\frac{\partial}{\partial t}\chi(t, v)\right| < \frac{K_2}{v^2}$$

It follows from this definition that for small t the numbers ν_t are bounded from below by some positive constant.

As an example, consider the following typical representation of the magnetic susceptibility in the volume L^D:

$$\chi_2(T, L) = cL^D \exp[-fL^{2D}(T - T_c(L))^2] + \eta(T, L) \tag{25}$$

with $c, f > 0$ real constants and $\eta(\cdot, L)$ analytic for $L < \infty$, locally uniformly convergent as $L \nearrow \infty$ [so that $\eta(\cdot, \infty)$ is analytic]. With $v = L^{-D}$, $t = [T - T_c(L)]/T_c(L)$, it is straightforward to show that

$$\chi(t, v) := \chi_2(T, L)$$

belongs to $\Psi_1^{(\omega)}(\mathcal{U})$ for some ω. Furthermore, $1/\nu_t \to 0$ as $t \to 0$. If $|T_c(L) - T_c| < dL^{-m}$ for some $d > 0$ and $m \geqslant D$, the same holds if we put $t = (T - T_c)/T_c$.

More generally, every function $\chi: \mathscr{U}^* \to \mathbf{R}$ of the form

$$\chi(t, v) = \frac{1}{v} f\left(\frac{t}{v}\right) + \tilde{\chi}(t, v) \tag{26}$$

belongs to $\Psi_1^{\omega}(\mathscr{U})$ with appropriate $\omega > 0$ if the following conditions are satisfied.

1a. $\tilde{\chi}(t, v) \in C^1(\mathscr{U}^*)$.

1b. $\tilde{\chi}(t, v)$ together with its (first) partial derivatives are uniformly bounded in $\mathscr{U}^*$.

2a. $f \in C^1(\mathbf{R})$ is a nonnegative function with $f(0) > 0$.

2b. $\lim_{x \to \pm\infty} |x|^{1+\varepsilon} f(x) = 0$ for some $\varepsilon > 0$.

2c. $(d/dx) f(x)$ is uniformly bounded on $\mathbf{R}$.

Any such function has the property that it "approaches δ" locally, i.e.,

$$\lim_{\varepsilon \to 0+} \lim_{v \to 0+} \int_{-\varepsilon}^{\varepsilon} dt\, \chi(t, v) > 0$$

and is finite. In this case the limits do not commute. An explicit example for such a function is

$$f(x) = \left(\frac{c}{\pi}\right)^{1/2} \exp(-cx^2), \qquad c > 0$$

with normalization

$$\int_{-\infty}^{\infty} dx\, f(x) = 1$$

After these preliminaries we now state the following volume dependence.

Lemma 3.1. Let $\omega > 0$, $\chi \in \Psi_1^{\omega}(\mathscr{U})$. There are $\delta, \varepsilon > 0$, and for every $t \neq 0$ there is $v_t > 0$ such that in $\mathscr{U}^*$ for all w, v, t with $v < \delta$ and $v_t w < |t| < \varepsilon v$,

$$\chi(t, v) > |\chi(t, w)|$$

In particular the lemma holds for $w = 0$, i.e.,

$$\chi(t, v) > |\chi(t, 0)|$$

This means that the susceptibility in that part of the transition region where $|t|/v < \varepsilon$ and $v < \delta$ is larger than in the infinite-volume limit, where $w = 0$.

Proof. Let $\chi \in \Psi_1^{\omega}(\mathcal{U})$, $\omega > 0$. Differentiability implies that

$$\chi(t, v) = \chi(0, v) + t \int_0^1 ds \frac{\partial}{\partial \eta} \chi(\eta, v) \Big|_{\eta = st}$$

With appropriate c_0, $K > 0$ we have

$$\chi(0, v) \geqslant \frac{c_0}{v}$$

and

$$\left| \frac{\partial}{\partial \eta} \chi(\eta, v) \right| < \frac{K}{v^2}$$

in $\mathcal{U}^*$. Hence

$$\chi(t, v) \geqslant \frac{c_0}{v} - \frac{|t| K}{v^2}$$

Furthermore, for every $t \neq 0$ there is $v_t > 0$ such that

$$|\chi(t, w)| \leqslant \omega$$

for all $w < |t|/v_t$. Finally, we choose $\varepsilon = c_0/(2K)$ and $\delta = c_0/(4\omega)$ and get for $v < \delta$ and $v_t w < |t| < \varepsilon v$

$$\chi(t, v) \geqslant \frac{c_0}{v} - \frac{\varepsilon K}{v} = \frac{c_0}{2v} > |\chi(t, w)|$$

Thus the lemma follows. ∎

Now we come to the second-order transition. In contrast to the first-order case, at a second-order transition the order parameter susceptibility can be divergent in the infinite-volume limit as the critical temperature is approached. This is described by the following definition.

Definition 3.2. For any $\gamma > 0$ we denote by $\Psi_2^{\gamma}(\mathcal{U})$ the set of functions $\chi: \mathcal{U}^* \to \mathbf{R}$ that are continuous and satisfy the following conditions.

1. There are constants $\mathscr{A}, K, \varepsilon > 0$ such that in $\mathscr{U}^*$

$$|\chi(t, 0) - \mathscr{A} |t|^{-\gamma}| \leqslant K |t|^{-\gamma+\varepsilon}$$

Furthermore, with appropriate $v, \mathscr{C} > 0$, we have, whenever $|t| > vv$,

$$\chi(t, v) \geqslant \mathscr{C}\chi(t, 0)$$

2. There are constants $\eta, \mathscr{B} > 0$ such that for $|t| < \eta v$

$$|\chi(t, v)| < \mathscr{B} v^{-\gamma}$$

The specific property for a second-order transition that the singular part of the free energy density behaves as a generalized homogeneous function implies for the susceptibility in a volume L^D a typical form like

$$\chi_2(T, L) = |T - T_c(L)|^{-\gamma} Q((T - T_c(L)) L^{1/\nu}) + \eta(T, L) \tag{27}$$

with some $\gamma > 0$. Here $\eta(\cdot, L)$ has similar analyticity properties as in (25) above, $\nu > 0$ is the critical exponent of the correlation length

$$\xi \sim |T - T_c|^{-\nu} \tag{28}$$

and Q is continuous and behaves as

$$\begin{aligned} \lim_{x \to 0} |x|^{-\gamma} Q(x) &= K > 0 \\ \lim_{x \to \pm\infty} Q(x) &= C > 0 \end{aligned} \tag{29}$$

The first equation expresses the absence of a nonanalyticity of χ_2 for finite L, the second one its presence in the infinite-volume case. With $t = [T - T_c(L)]/T_c(L)$, $v = L^{-1/\nu}$, and

$$\chi(t, v) := \chi_2(T, L)$$

we see that χ belongs to $\Psi_2^{\gamma}(\mathscr{U})$ for some γ.

More generally, every function $\chi: \mathscr{U}^* \to \mathbf{R}$ of the form

$$\chi(t, v) = \frac{1}{v^{\gamma}} f\left(\frac{t}{v}\right) + \tilde{\chi}(t, v) \tag{30}$$

with $\gamma > 0$ belongs to some $\Psi_2^{\gamma}(\mathscr{U})$ if the following conditions are satisfied.

1. $\tilde{\chi}(t, v) \in C^1(\mathscr{U}^*)$.

2a. $f \in C^1(\mathbf{R})$ and $f(0) > 0$.

2b. $\lim_{x \to \pm\infty} |x|^\gamma f(x) = C$ for some finite $C > 0$.

Compared to the first-order case (26), the essential difference comes from property (2b).

As an example,

$$\chi(t, v) = (t^2 + v^2)^{-(m/2)}, \qquad m > 0$$

belongs to the class Ψ_2^m.

For these functions, we have the following in contrast to Lemma 3.1.

Lemma 3.2. Let $\gamma > 0$ and $\chi \in \Psi_2^\gamma(\mathscr{U})$. There are constants $v, \varepsilon > 0$ such that for all t, v, w with $vw < |t| < \varepsilon v$,

$$|\chi(t, v)| < \chi(t, w)$$

The inequality is always true if $w = 0$, i.e., the susceptibility is always smaller than in the infinite-volume limit as long as we are in the critical region $|t|/v < \varepsilon$.

Proof. Let $\chi \in \Psi_2^\gamma(\mathscr{U})$, $\gamma > 0$. There are numbers $\mathscr{C}$, $\mathscr{D}$, $v > 0$ such that in $\mathscr{U}^*$ for $|t| > vw$

$$\chi(t, w) > \mathscr{C}\chi(t, 0) > \mathscr{D}\,|t|^{-\gamma}$$

Furthermore, there are $\eta, \mathscr{B} > 0$ such that for $|t| < \eta v$

$$|\chi(t, v)| < \mathscr{B} v^{-\gamma}$$

We choose $\varepsilon = \min(\eta, (\mathscr{D}/\mathscr{B})^{1/\gamma})$ and get for $vw < |t| < \varepsilon v$

$$|\chi(t, v)| < \mathscr{B} v^{-\gamma} < \mathscr{B}\left(\frac{\varepsilon}{|t|}\right)^\gamma < \frac{\mathscr{B}\varepsilon^\gamma}{\mathscr{D}}\chi(t, w) < \chi(t, w)$$

This proves the lemma. ∎

3.2. The Effective Potential

Let us briefly discuss another method to determine the nature of a transition that will be of use later on. For definiteness we come back to the

N-component scalar model as described in Section 2. A possible way to define an effective potential is by

$$V \cdot V_{\text{eff}}(M) = -\Gamma(M)|_{M=\text{const}} \tag{31}$$

where V denotes the volume and $\Gamma(M)$ is defined by (6). In the symmetric phase and in the infinite-volume limit, V_{eff} has to be convex. In practice, the right-hand side of (31) is obtained as an expansion about $M=0$. In the linked cluster expansion the coefficients can be expressed in terms of 1PI susceptibilities $\chi_n^{1\text{PI}}$. They are obtained as series representation in κ of the truncated susceptibilities by keeping only those graphs that are $1\text{PI}^{(9)}$ (1PI graphs are graphs that cannot become disconnected by cutting off one of their internal lines). Up to a constant we obtain

$$V_{\text{eff}}(M) = \frac{1}{2}\frac{1-4D\kappa\chi_2^{1\text{PI}}}{\chi_2^{1\text{PI}}}M^2 - \frac{1}{4!}\frac{\chi_4^{1\text{PI}}}{(\chi_2^{1\text{PI}})^4}(M^2)^2 - \frac{1}{6!}\frac{1}{(\chi_2^{1\text{PI}})^6}\left(\chi_6^{1\text{PI}} - \frac{10(\chi_4^{1\text{PI}})^2}{\chi_2^{1\text{PI}}}\right)(M^2)^3 + O(M^8) \tag{32}$$

Any nonconvex shape of V_{eff} in the infinite-volume limit must be an artifact of the approximation scheme. In a finite volume, however, a nonconvex shape in the symmetric phase signals a first-order transition, whereas a convex shape is compatible with a second-order transition. An estimate of the critical coupling is then obtained by a root of the coefficient of M^2 in the second-order case, and by degenerate values of V_{eff} at the trivial and nontrivial minima in the first-order case. In our applications (see Section 4) we have calculated the 1PI susceptibilities $\chi_{2n}^{1\text{PI}}$ up to 16th order in κ in a finite volume for $n=1, 2, 3$.

4. APPLICATIONS TO SCALAR $O(N)$ MODELS WITH Φ^4 AND Φ^6-POINT COUPLINGS

In this section we apply the methods discussed in the previous sections to the three-dimensional $O(N)$ symmetric scalar model with $N=1$ and $N=4$. The model is described on a lattice Λ by the partition function

$$Z(\kappa, \lambda, \sigma) = \int \prod_{x \in \Lambda} d^N\Phi(x) \exp\left[2\kappa \sum_{x,y\,\text{NN}} \Phi(x)\cdot\Phi(y) - \sum_x \mathring{S}(\Phi(x), \lambda, \sigma)\right] \tag{33}$$

where the first sum of the exponential runs over unordered pairs of nearest neighbor lattice sites, and the ultralocal part $\mathring{S}$ is given by

$$\mathring{S}(\Phi, \lambda, \sigma) = \Phi^2 + \lambda(\Phi^2 - 1)^2 + \sigma(\Phi^2 - 1)^3 \tag{34}$$

with $\sigma > 0$ or $\sigma = 0$ and $\lambda \geqslant 0$. In statistical physics this model is known under the name Blume–Capel model.[22, 23] In contrast to the pure quartic interaction, which only admits second-order transitions, the action (34) allows a richer phase structure with regions of first- and second-order transitions due to the additional Φ^6 interaction. The case of $\lambda = 3\sigma$ corresponds to a pure Φ^6-theory, whereas $\lambda < 3\sigma$ implies a negative quartic coupling.

4.1. Preliminaries

To get a first estimate of the phase structure we consider the case of large couplings λ and σ. For finite coupling constants we invoke a hopping-mean-field analysis.

The Large-Coupling Limit. To study the limit of large couplings, we set $\lambda = \alpha\sigma$ and send σ to infinity with α and κ kept finite and fixed. This limit is discussed for more general contact terms in Appendix A. The discussion is based on a saddle-point integration. As a result we obtain the following behavior in dependence on α. For $\alpha > 1$ and $\alpha < -3$ we obtain $O(N)$ Heisenberg models (Ising model for $N = 1$). The range of $-3 < \alpha < 1$ leads to complete disordering with no phase transition at any finite κ. The cases of $\alpha = -1$ and $\alpha = 3$ are peculiar. The resulting actions describe "diluted" $O(N)$ models, with particular values of the couplings. If the large-coupling limit is performed term by term in the HPE series it can be shown that at least for $N \geqslant 2$ the resulting actions again belong to the unversality class of $O(N)$ Heisenberg models.

A Hopping-Mean-Field Analysis. To get a first estimate of the phase structure at *finite couplings*, it is instructive to start with a mean-field analysis. Together with the convexity of the exponential and the positivity of the measure this ansatz leads to a complete factorization of the partition function. The hopping-mean-field estimate for the free energy is then derived as follows. Let us define $\mathring{x}$ by

$$\exp \mathring{x}(H) = \int d^N\Phi \exp[-\mathring{S}(\Phi, \lambda, \sigma) + H \cdot \Phi]$$

and the expectation value $\langle F \rangle_H$ of an observable F according to

$$\langle F(\Phi) \rangle_H = \exp[-|\Lambda| \mathring{x}(H)] \times \int \prod_{x \in \Lambda} \left(d^N \Phi(x) \exp\left[-\sum_x \mathring{S}(\Phi) + H \cdot \Phi \right] \right) F(\Phi)$$

Here $|\Lambda|$ denotes the lattice volume and $H \in \mathbb{R}^N$ is an auxiliary field. Note that $\mathring{x}$ defined in this way agrees with $\mathring{W}$ as introduced in Section 2. In particular, for every integer n,

$$\mathring{v}^c_{2n}(\lambda, \sigma) = \frac{\partial^{2n}}{\partial H_1^{2n}} \mathring{x}(H) \Big|_{H=0}$$

[compare to (11)]. For simplicity, where no confusion can arise, we only indicate the dependence on H. We get

$$\begin{aligned} Z(\kappa, \lambda, \sigma) &= \left\langle \exp\left[2\kappa \sum_{x, y \text{ NN}} \Phi(x) \cdot \Phi(y) \right] \right\rangle_H \\ &\geqslant \exp\left\langle 2\kappa \sum_{x, y \text{ NN}} \Phi(x) \cdot \Phi(y) \right\rangle_H \\ &= \exp[-|\Lambda| \bar{f}(H)] \end{aligned}$$

with

$$\bar{f}(H) = -(\mathring{x}(H) + 6\kappa(\nabla_H \mathring{x}(H))^2 - H \cdot \nabla_H \mathring{x}(H))$$

An upper bound on the true free energy density f is thus given by

$$f \leqslant \inf_H \bar{f}(H) \tag{35}$$

A vanishing $H_0 = 0$ is always a solution of the corresponding mean-field equation

$$\partial_H \bar{f}(H_0) = -\partial_H^2 \mathring{x}(H_0)[12\kappa \, \partial_H \mathring{x}(H_0) - H_0] = 0$$

where the derivative is in the direction of H, and $H_0 = 0$ is a local minimum of $\bar{f}$, if

$$\partial_H^2 \bar{f} = \partial_H^2 \mathring{x}(H_0)[1 - 12\kappa \, \partial_H^2 \mathring{x}(0)] > 0 \tag{36}$$

In particular, for small hopping parameter κ the model is always in the symmetric phase. This form of mean-field analysis is identical to the tree level of the hopping parameter expansion. The hopping-mean-field analysis has been used, for example, in ref. 24 under the name *molecular field approximation* to investigate the phase structure of the spin-1 Ising model and to compare it to ^{3}He–^{4}He mixtures.

It can easily be shown that the Lebowitz inequality (cf., e.g., refs. 25, 26)

$$\partial_H^3 \mathring{x}(H) < 0 \qquad \text{for all} \quad H > 0$$

together with $\partial_H^2 \mathring{x}(H) > 0$ for all H ensures that $H_0 = 0$ is the absolute minimum of $\bar{f}$. The Lebowitz inequality holds in any case for $\lambda \geqslant 3\sigma$. Equality in (36) along with

$$\partial_H^4 \bar{f}(0) > 0 \tag{37}$$

locates a second-order phase transition to the spontaneously broken phase at

$$\kappa_c(\lambda, \sigma) = \frac{1}{12\mathring{v}_2^c(\lambda, \sigma)}$$

Tricritical points are identified by an equality in (37) and

$$\partial_H^6 \bar{f}(0) > 0 \tag{38}$$

i.e.,

$$\mathring{v}_4^c(\lambda, \sigma) = 0 \qquad \text{and} \qquad \mathring{v}_6^c(\lambda, \sigma) < 0$$

We notice that these conditions imply a vanishing two- and four-point coupling in the effective potential V_{eff}, Eq. (32), evaluated to tree level in the HPE, i.e., in the hopping-mean-field approximation. Thus the criterion for tricriticality reduces to the familiar one. If we had used the *classical* potential (34) instead, this would have led to a location of the tricritical line in the bare coupling constant space at $\lambda = 3\sigma$.

In Table I we list some results for the $O(4)$ model on the location of the tricritical line in the (λ, σ) space for several values of α.

The *tricritical exponents* in hopping-mean-field establish the results of the most naive mean-field analysis with the effective potential replaced by the classical potential. They are $\alpha = 1/2$, $\beta = 1/4$, $\gamma = 1$, $\delta = 5$, and $\nu = 1/2$. From the Ginzburg criterion one may expect that the only chance where

Table I. Mean-Field Tricritical Line for the $O(4)$ Model on the Three-Dimensional Hypercubic Lattice[a]

α	$\lambda = \alpha\sigma$	σ	$\bar{\sigma}$
1/1.05	128.199	134.609	−0.7245305
1/1.1	53.040	58.344	−0.6875585
1/1.2	21.822	26.286	−0.5920738
1/1.3	13.252	17.228	−0.5193738
1/1.5	7.315	10.973	−0.4451270
1/2.0	3.401	6.802	−0.3839411
1/5.0	0.788	3.941	−0.3407590
1/10.0	0.344	3.494	−0.3345469
1/100.0	0.031	3.081	−0.3306763
−1/10.0	−0.273	2.731	−0.3284753
−1/1.1	−1.391	1.530	−0.3519023
−1.0	−1.472	1.472	−0.3581768
−2.0	−2.948	1.474	−0.5106579
−3/1.2	−7.561	3.024	−0.6827047
−3/1.1	−17.678	6.482	−0.7259408

[a] The line is defined by $v_4^c = 0$ and $v_6^c < 0$; $\bar{\sigma}$ is defined by $\bar{\sigma} = v_6^c/[5(v_2^c)^3]$.

a mean-field type of analysis may lead to reliable predictions of the singular behavior in *three* dimensions is *at* tricriticality. In fact, the susceptibility comes out as volume independent along the tricritical line (cf. Section 4.3 below) when it is determined by the HPE analysis. A mean-field analysis is volume independent by construction.

4.2. Infinite-Volume Analysis at Finite Couplings

So far we have studied the phase structure in the large-coupling limit and in a mean-field analysis for finite couplings. Next we utilize the linked cluster expansions for a more thorough study. Susceptibilities are represented as convergent power series in the hopping parameter, such as the $2n$-point functions

$$\chi_{2n}(\kappa, \lambda, \sigma) = \sum_{\mu \geq 0} a_\mu^{(2n)}(\lambda, \sigma)\, \kappa^\mu \tag{39}$$

and similarly for weighted correlations. These series have been computed to 20th order in κ for $n = 1$, to 18th order for $n = 2$, and to 16th order for $n = 3$, both in a finite and an infinite volume. In the infinite volume, the coefficients of the series we have explicitly calculated are of equal sign for

each series. Under the assumption that this behavior continues to all orders in κ, we identify the radius of convergence $\kappa_c(\lambda, \sigma)$ with the singularity closest to the origin on the positive real axis, hence with the physical singularity at the phase transition, independently of the order of the transition.

Well-developed methods are known for obtaining critical data from the high-order coefficients of high-temperature series.[4, 21] The critical point $\kappa_c(\lambda, \sigma)$ is identified by the ratio criterion applied to the coefficients $a_\mu^{(2n)}(\lambda, \sigma)$. The best choice is the two-point susceptibility, because its series is available to the highest order. The obliged regression toward large μ is done according to

$$q_\mu := \left| \frac{a_\mu^{(2)}}{a_{\mu-1}^{(2)}} \right| = \frac{1}{\kappa_c} \left(1 + \frac{c_1}{\mu^{\omega_1}} + O(\mu^{-\omega_2}) \right) \tag{40}$$

with $\omega_2 > \omega_1 > 0$, and c_1 as fit parameter chosen according to the best χ^2/df fit. This procedure is eventually supplemented by a shift of the weak antiferromagnetic singularity at $-\kappa_c$ to $-\infty$, an improved estimator fit, and other known techniques, such as Padé methods. We know that $\omega_1 = 1$ for a leading pole or branch point singularity on the real axis, i.e., for

$$\chi_2 \simeq \mathscr{A}(\kappa_c - \kappa)^{-\gamma} \qquad \text{as} \qquad \kappa \nearrow \kappa_c$$

with $\gamma > 0$ and $\gamma \neq 1$, and $\omega_1 > 1$ for $\gamma = 1$. For a second-order transition, an alternative way to determine the critical point is given by the smallest real solution of

$$12\kappa_c \chi_2^{1\mathrm{PI}}(\kappa_c) = 1$$

as proposed in ref. 9. This condition is equivalent to the identification of the phase transition as a zero of the quadratic coefficient of the effective potential; cf. (32). It turns out to be the most convenient way to determine the radius of convergence leading to the highest precision in κ_c. The lowest precision obtained in this way lies within 4–5 digits. Once κ_c is determined we obtain the critical exponent γ from

$$1 + \mu(\kappa_c q_\mu - 1) = \gamma + \frac{c_2}{\mu^{\omega_3}} + o(\mu^{-\omega_3}) \tag{41}$$

with ω_3 and c_2 as fit parameters. In a similar way, the critical exponent ν is obtained by replacing the series of χ_2 by that of m_R^{-2}; cf. (8).

A measurement of critical exponents like γ, ν, η leads to a qualitative plot of the phase structure in the (λ, σ) half-plane as shown in Fig. 2. The solid line represents the boundary $\lambda = \lambda_t(\sigma)$ between the second- and first-order regions. To the left of this tricritical line the phase transition is of second order. Here, except for the origin $\lambda = \sigma = 0$, we obtain one universality class for every N with plateaus of critical exponents, with values of the N-component Heisenberg model (cf., e.g., ref. 9 for a recent list of those exponents). It is remarkable that this range considerably extends the "Lebowitz domain" $\lambda \geqslant 3\sigma$, where the action is convex and therefore γ is not less than 1.[26] In particular, it includes the full range of $\lambda < -3\sigma$. In passing we mention that for $\lambda \geqslant 0$ the presence of a small nonvanishing Φ^6 interaction, that is, $\sigma > 0$, considerably accelerates the convergence of the high-temperature series compared to the case $\sigma = 0$, i.e., the nonuniversal remainder of (40) becomes smaller.

Except for the values of the critical exponents, the phase structure qualitatvely confirms the mean-field analysis of the last subsection. As the tricritical line $\lambda = \lambda_t(\sigma)$ is approached, the exponents γ and ν drop continuously from their values in the Heisenberg models to the Gaussian values, where the tricritical line is crossed, and further to zero. The smooth interpolation between the different exponents is an artifact of the truncation of the power series expansions at high, but finite order in κ.

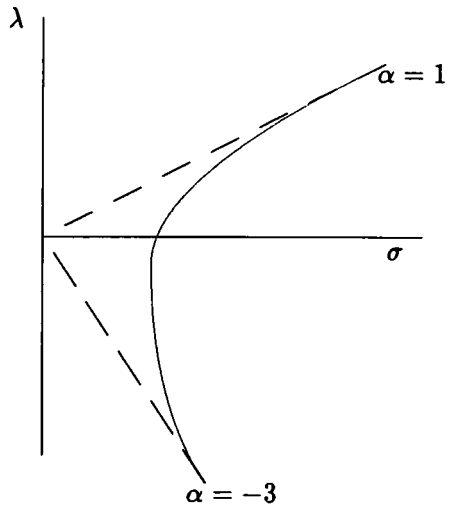

Fig. 2. Qualitative plot of the phase structure of $O(N)$ lattice models in three dimensions. The dashed curves give the lines $\lambda = \alpha\sigma$ with $\alpha = 1$ and $\alpha = -3$. The solid curve represents the tricritical line $\lambda_t(\sigma)$. To the left of it the phase transition is of second-order, to the right of it, first order.

It was already pointed out in ref. 9 that various universality classes lead to smearing effects at finite order due to an "interference" of various universality domains. The most pronounced plateau structure is obtained for $\nu\eta$, the critical exponent of the wave function renormalization constant Z_R, (9).

In Fig. 3 we show the results on the exponent $\nu\eta$ for the $O(4)$ model, obtained from the 20th-order susceptibility series of χ_2 and μ_2, (5), for various σ along the ray $\lambda = (1/2)\,\sigma$. There is a well-established plateau at the left part of the plot corresponding to the universality class of the Heisenberg model. The plateau at the right part is compatible with a range of first-order transitions; all exponents γ, ν, η vanish within the error bars. Hence they are compatible with a finite correlation length at κ_c. The stability of the extrapolated convergence radius κ_c under a variation of the truncation of the series suggests that there is really a first-order transition rather than a mere crossover phenomenon. We would like to identify the left boundary of this plateau as the tricritical point. This gives us an estimate of about $\sigma_t \simeq 9.0$. The indicated errors in Fig. 3 are obtained as discussed in connection with (41). The smearing effect does not allow for a more precise location of the tricritical point. To get a clearer identification of the first-order transition region and a better localization of the tricritical point it is natural to perform a finite-size scaling analysis, which is the topic of the next section.

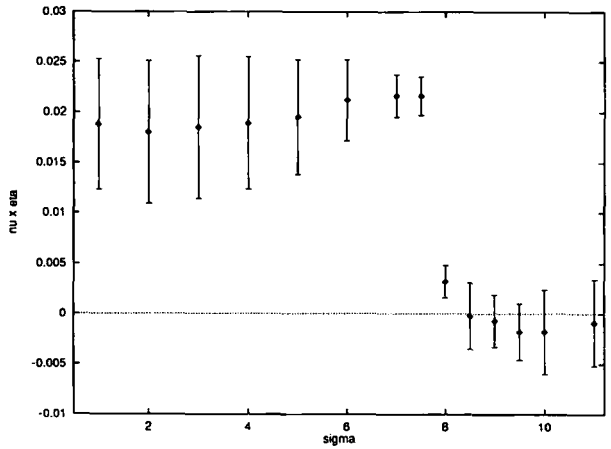

Fig. 3. Critical exponent $\nu\eta$ of the wave function renormalization constant Z_R for the 3D $O(4)$ model, obtained from the 20th-order susceptibility series for various σ along the ray $\lambda = (1/2)\,\sigma$. The tricritical point is at $\sigma_t \simeq 9.0$. The mean-field estimate gives $\sigma_t = 6.8$.

4.3. Results of the Finite-Size Scaling Analysis

In Section 3 we formulated monotony criteria for response functions χ in the scaling region. In absolute value, increase in volume implies a second-order transition, decrease in volume a first-order one. The response functions have to be calculated at some $\tilde{\kappa}$ close to, but not at the critical point κ_c for two volumes. The value of $\tilde{\kappa}$ should be chosen sufficiently close to the (volume-dependent) transition point to satisfy the conditions of the monotony criteria, and sufficiently apart from $\kappa_c(L)$ to allow the use of the truncated series representation. In our case in turned out that a choice of $\tilde{\kappa} = 0.98\kappa_c(\lambda, \sigma, L_l = \infty)$ fulfills both restrictions for first- and second-order transitions. In general it might be safer if $\tilde{\kappa}$ is chosen either to the left or to the right of both peaks, i.e., in our case smaller than $\min(\kappa_c(L_l), \kappa_c(L_s))$, in order for the conditions for the monotony criteria to apply.

The volumes should be sufficiently large in lattice units to guarantee the applicability of the finite-size scaling ansatz for χ. Beyond this generic condition the following restrictions arise from the monotony criterion. The smaller one of the two volumes should satisfy $L^x |\tilde{\kappa} - \kappa_c| \lesssim 1$ with $x = 1/\nu$ or $x = 3$, which implies an upper bound on L for given $\tilde{\kappa}$. In practice we have chosen this L between 4 and 12. In the context of the HPE the larger one of the two volumes may be set to infinity. The advantage of this choice is that in the first-order case, decrease in volume holds all over the scaling region. In Monte Carlo simulations the second volume is necessarily finite. In this case L should be large enough so that $\tilde{\kappa}$ lies outside the small neighborhood of κ_c where χ is increasing in the first-order case as well. The critical point $\kappa_c(\lambda, \sigma)$, which enters the inequalities on L and $\tilde{\kappa}$, is determined as the radius of convergence in the infinite volume as described above.

We use the two-point susceptibility because its series is available to the highest order in κ. For given couplings λ and σ

$$\chi_2^{(M)}(\tilde{\kappa}, \lambda, \sigma; L) = \sum_{\mu=0}^{M} a_\mu^{(2)}(\lambda, \sigma; L)\, \tilde{\kappa}^\mu \tag{42}$$

denotes the two-point susceptibility truncated at order M. With

$$r_M(\lambda, \sigma; L) := 1 - \frac{\chi_2^{(M)}(\tilde{\kappa}, \lambda, \sigma; L)}{\chi_2^{(M)}(\tilde{\kappa}, \lambda, \sigma; \infty)} \tag{43}$$

we know that $r_\infty(\cdot; L) > 0$ for second-order and $r_\infty(\cdot; L) < 0$ for first-order transitions if L lies within the bounds as explained above. The convergence of the series (42) as $M \to \infty$ ensures the same behavior for finite, but sufficiently large M.

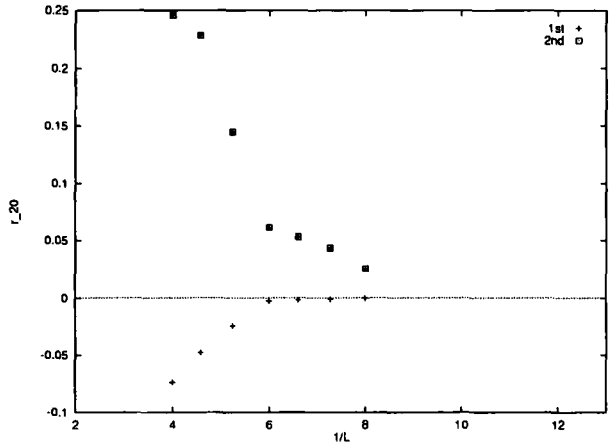

Fig. 4. Dependence of the ratio $r_{20}(\lambda, \sigma; L)$, as defined by (43), on $L=(L_1L_2L_3)^{1/3}$, with the example of the $\mathbb{Z}_2$ model. Two points of the phase space have been chosen. (1) (+) $\lambda=15/1.1$ and $\sigma=15$. The transition is of first order, $r_{20}<0$. (2) (□) $\lambda=3$ and $\sigma=1$. The transition is of second order, $r_{20}>0$.

Figure 4 shows an application of the monotony criteria to the one-component model. We have plotted the volume dependence of the ratio $r_M(\lambda, \sigma; L)$ for a truncation at order $M=20$ and for various lattice sizes $L=(L_1L_2L_3)^{1/3}$ at two points of the bare coupling constant space. One point is well inside the first-order region, the other one well inside the second-order part of the phase diagram; the different areas have been identified by the infinite-volume series as discussed in the last subsection. Clearly the sign of $r_{20}(\cdot; L)$ is different in both regions of phase space. It is positive for the second-order transition and negative for the first-order transition. The approach to the infinite-volume limit where $r_M(\cdot; \infty)=0$ is fast.

Next we want to demonstrate how one can utilize the finite-volume criteria with HPE to get a better localization of the tricritical region. Let us consider the $O(4)$ model and determine the behavior of the ratio r_M along the line $\lambda=(1/2)\sigma$. From the infinite-volume analysis of the last subsection we obtained $\sigma_t \simeq 9.0$ as an estimate for the tricritical coupling σ_t.

Since $r_M(\lambda, \sigma; L)>0$ for second-order and <0 for first-order transitions, the tricritical point should be localized at the zero of $r_M(\lambda, \sigma; L)$ between these two ranges [with nonvanishing slope, i.e., $\partial r_M(\sigma/2, \sigma; L)/\partial\sigma \neq 0$], suitably extrapolated to $M, L \to \infty$.

Figure 5 shows the ratio $r_M(\sigma/2, \sigma; L)$ as function of σ for $L=4$ and various M between 0 (corresponding to the mean-field approximation) and 20. The intersections of the curves with the $r=0$ axis lie in the range

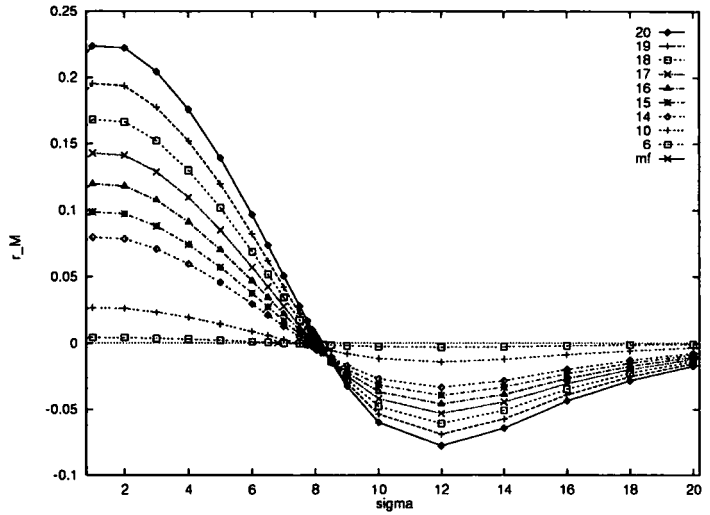

Fig. 5. The ratio $r_M(\lambda, \sigma; L)$ as a function of σ for $\lambda = \sigma/2$ and $L = 4$, i.e., on a $4 \times 4 \times 4$ lattice.

of $8 \leqslant \sigma \leqslant 8.5$. The zeros $\sigma_M(L)$, defined by $r_M(\sigma_M(L)/2, \sigma_M(L); L) = 0$, depend on the order M at which the susceptibility series of χ_2 have been truncated and on the lattice size L. The dependence on L for fixed M of $r_M(\lambda, \sigma; L)$ is shown in Fig. 6.

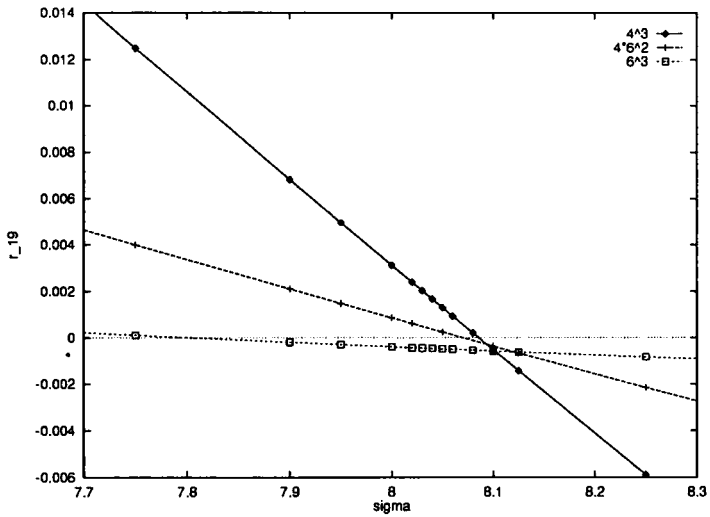

Fig. 6. Dependence of the ratio $r_{19}(\sigma/2, \sigma; L)$ as defined by (43) on σ for various volumes.

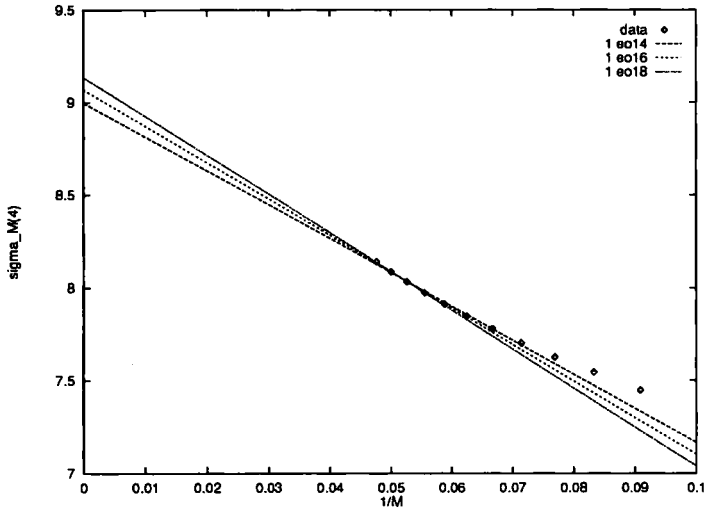

Fig. 7. The solution $\sigma_M(L)$ of the equation $r_M(\sigma_M(L)/2, \sigma_M(L); L) = 0$ for $L = 4$, plotted against $1/M$, where M is the order of truncation of the suceptibility series. Regression is shown as a linear function of $1/M$ for $M \geqslant M_{\min}$ with $M_{\min} = 14, 16, 18$.

Thus a final localization of the tricritical coupling σ_t needs an extrapolation in L and M to infinity. Clearly the extrapolations are not independent of each other. We should expect that a comparision of two ratios is sensible, i.e.,

$$r_M(\cdot; L) \simeq r_{M'}(\cdot; L') \tag{44}$$

if lattice sizes L, L' and truncations M, M' satisfy

$$\frac{M}{L} = \frac{M'}{L'} \tag{45}$$

The reason is that M/L is the maximal number of times a graph contributing to the series of $\chi_2^{(M)}(\cdot; L)$ can wind around the volume. Then Eq. (45) ensures that the remaining L dependence becomes independent of M for sufficiently large M.

Figure 7 shows the data $\sigma_M(L)$ obtained on a 4^3-lattice ($L = 4$) and for $11 \leqslant M \leqslant 20$ as a function of $1/M$. The curves show the regression

$$\sigma_M(4) = \sigma_t(M_{\min}, L = 4) + \frac{\delta(M_{\min})}{M}$$

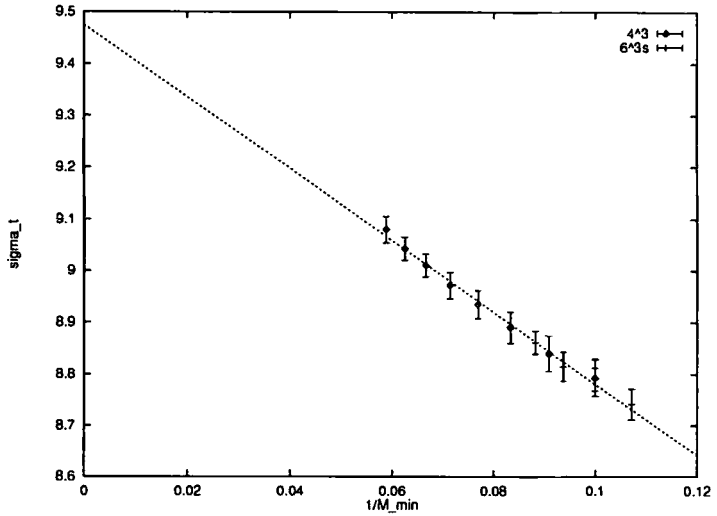

Fig. 8. The "scaled" solution $\sigma_t(M_{\min} L/4, L)$ plotted against $1/M_{\min}$ for $L=4$ and $L=6$. Within the error bars, the data are on a straight line, thus confirming the assumptions made in connection with Eqs. (44) and (45). Linear regression in $1/M_{\min}$ gives the tricritical point.

as obtained for $M_{\min} \leqslant M \leqslant 20$ and for $M_{\min} = 14, 16, 18$. In Fig. 8 we show the second regression for the resulting $\sigma_t(M_{\min} L/4, L)$ in $1/M_{\min}$ for $L=4, 6$,

$$\sigma_t\left(M_{\min}\frac{L}{4}, L\right) = \sigma_t + \frac{\varepsilon}{M_{\min}}$$

leading to the final prediction of σ_t. We have scaled the adjusted $M_{\min}$ according to (45). Note that both data sets, on the 4^3- and on the 6^3-lattice, fall on the same straight line within the error bars. We obtain

$$\sigma_t = 9.454(49) \tag{46}$$

In passing we remark that the accuracy of σ_t has been increased by at least one order of magnitude compared to the infinite-volume analysis (Fig. 3). It should be noticed that the volume independence of χ_2 in the scaling region of the tricritical point just confirms the validity of a mean-field analysis of tricritical exponents. A mean-field analysis is volume independent by construction. The expected volume independence of χ_2 is confirmed within the error bars. The validity of the mean-field analysis was also found by Baker and Johnson[27] in the large-coupling limit of the

Blume–Capel model in four dimensions and by Hara *et al.*[28] for dimensions larger than four.

In the remainder of this section we discuss the volume dependence of the radius of convergence and of the effective potential.

Shift and Scaling of $\kappa_c(\lambda, \sigma; L)$. We define $\kappa_c(\lambda, \sigma; L)$ in the finite and infinite volume as the radius of convergence of the susceptibility series, in particular of χ_2, which is known including the 20th order. Some data for $\kappa_c(L)$ are listed in Table II for the three-dimensional $O(1)$ and $O(4)$ models. The couplings (λ, σ) for each N $(N=1, 4)$ have been chosen deep in the first-order transition region.

From a finite-size scaling analysis one expects (cf. Section 3) that the data should fit with a regression in L according to

$$\ln |\kappa_c(\cdot; L) - \kappa_c(\cdot; \infty)| \simeq \ln c - y_T \ln L$$

for large L, with some constant c and a critical exponent y_T. For the $\mathbb{Z}_2$ model we obtain in the first-order transition region $(\lambda = 15/1.1, \sigma = 15.0)$ according to Table II

$$\ln c = 4.57(57), \qquad y_T = 6.21(32)$$

with $\chi^2/df = 0.025$. Thus the scaling behavior is consistent with $y_T = 2D = 6$. It confirms the behavior which has been predicted for the shift of the critical coupling determined as the maximum of the susceptibility in a

Table II. Radius of Convergence $\kappa_c(L)$ of the HPE Series for the First-Order Region[a]

	$\kappa_c(L)$	
L	$\mathbb{Z}_2$ $(\lambda = 13.64, \sigma = 15.0)$	$O(4)$ $(\lambda = 6.0, \sigma = 12.0)$
∞	0.51047(1)	0.84462(10)
4	0.49381	0.79531
6	0.50886	0.83851
8	0.51025	0.84416
10	0.51047	0.84436
12	0.51047	0.84447

[a] It is determined from the two-point susceptibility series, as described in Section 4.2. Data are given for the 3D $\mathbb{Z}_2$ and $O(4)$ models for various volumes L^3.

class of models which cover the $\mathbb{Z}_2$ model.[20] Note that it is in disagreement with the Gaussian two-peak model[18] predicting a leading finite-size correction proportional to L^{-D}, which one might have expected.

The same scaling behavior is found for the $O(4)$ model in the first-order transition region. Here we get (Table II)

$$\ln c = 4.57(120), \qquad y_T = 5.55(59)$$

Thus a leading correction proportional to L^{-3} lies clearly outside the error bars. This result is remarkable, because the $O(4)$ model (which is a Heisenberg model in the large-coupling limit) is not covered by the analysis of Borgs *et al.*[19,20] Hence the vanishing of the coefficient of the linear term in a large-volume expansion of the susceptibilities in powers of $1/L^3$ seems to be a universal feature of a large class of models.

A measurement of the scaling behavior of $\kappa_c(L)$ in the second-order region of the $O(4)$ model was not conclusive, because the shift of κ_c occurs in the fourth or fifth digits, hence the finite-size effect is hidden in the error. In the second-order region of the $\mathbb{Z}_2$ model we measure a scaling which is best fitted by an ansatz (cf. Table III)

$$\kappa_c(\cdot; L) = \kappa_c(\cdot; \infty) + \frac{c}{L^{y_T}}$$

with $y_T = 2/\nu$, and

$$\ln c = -2.25(129), \qquad y_T = 2.83(59)$$

with $\chi_2/df = 0.1$. From a renormalization group analysis one expects a leading scaling correction proportional to $L^{-1/\nu}$. Also here the finite-size effect is not large compared to the error in κ_c; thus the disagreement with

Table III. Radius of Convergence $\kappa_c(L)$ of the HPE Series for the Second-Order Region in the $\mathbb{Z}_2$ Model for Various Volumes L^3

L	$\kappa_c(L)$ ($\lambda = 3.0, \sigma = 1.0$)
∞	0.17316(4)
6	0.17393
8	0.17339
10	0.17327
12	0.17327

an $L^{-1/\nu}$ behavior may be due to the errors in κ_c and the uncertainty in the involved extrapolations.

We conclude the discussion of $\kappa_c(L)$ with a conjecture concerning the monotony behavior.

Monotony in $\kappa_c(L)$. The results of Table II for $\kappa_c(L)$ exhibit a further characteristic distinction between first- and second-order transitions. Since we are not aware of a general proof, we leave it as a conjecture.

Conjecture. The convergence radius $\kappa_c(L)$ of the series expansions is monotonically decreasing with L for second-order transitions, and monotonically increasing for first-order transitions.

The Effective Potential as Function of L. Similarly we have measured V_{eff}, Eq. (32), for two points well inside the supposed first- and second-order transition regions of the $O(4)$ model ($\lambda = 6.0, \sigma = 12.0$ and $\lambda = 0.\overline{90}, \sigma = 1.0$, respectively). The χ_{2n}^{1PI} entering Eq. (32) have been evaluated to 16th order in κ for $n = 1, 2, 3$ in a finite and an infinite volume. For the second-order point $\lambda = 0.\overline{90}, \sigma = 1.0$ and for volumes L^3 with $L = 4$, 6, and ∞, V_{eff} is convex in the symmetric phase up to a resolution of 10^{-8}.

In the first-order case (Fig. 9) V_{eff} is nonconvex in the symmetric phase with a barrier height decreasing with increasing L. The three curves

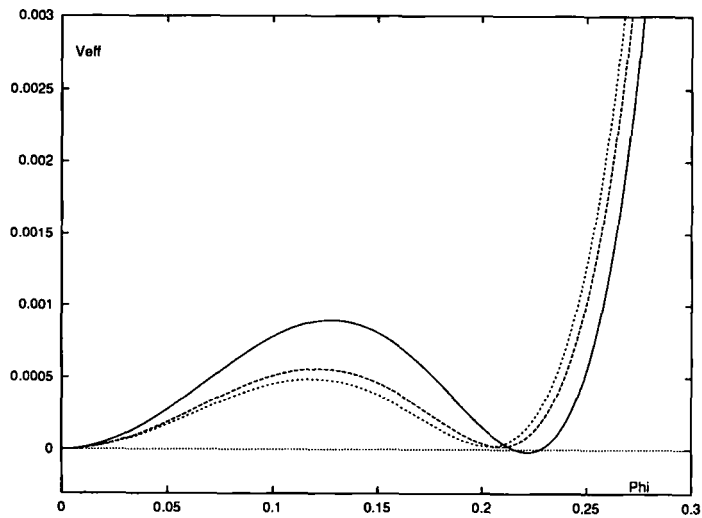

Fig. 9. Volume dependence of the effective potential $V_{\text{eff}}(\Phi)$ on lattices with varying size L^3. The barrier height decreases with L. The curves are obtained for $L = 4$, 6, ∞. The parameters are $\lambda = 6.0, \sigma = 12.0$ in the 3D $O(4)$ model.

correspond to a 4^3, 6^3, and ∞^3 lattice, respectively. Note that the nonconvex shape, which is even seen for the ∞^3 lattice (lowest barrier in Fig. 9), must be attributed to the approximation scheme, i.e., to the truncation at order $M = 16$. (As mentioned above, the truncation of the series expansion acts similarly to a finite-volume cutoff. The finite volume leads to a nonconvex shape only in the first-order case. Thus it is not surprising that we find a convex shape in the symmetric phase for all volumes in the second-order case, in spite of the same truncation in M.)

The coexistence of minima leading to the same value of V_{eff} defines a critical coupling $\tilde{\kappa}_c(L)$ which need not agree with the finite-volume convergence radius $\kappa_c(L)$ unless the truncated expansions of $V_{\text{eff}}(\Phi)$ in Φ and of χ_{2n}^{1PI} in κ are extrapolated to infinity. For parameters chosen as in Fig. 9 we find $\tilde{\kappa}_c(4) = 0.8311$, $\tilde{\kappa}_c(6) = 0.8475$, and $\tilde{\kappa}_c(\infty) = 0.8488$, in contrast to $\kappa_c(4) = 0.79531$, $\kappa_c(6) = 0.83851$, and $\kappa_c(\infty) = 0.84462$ (cf. Table II), determined as the radius of convergence of the series expansions, extrapolated to infinite M.

Tricritical Parameters from V_{eff}. Vanishing coefficients of the Φ^2 and Φ^4-terms associated with a qualitative change in the shape of V_{eff} provide a further possibility for localizing the tricritical couplings. The analytical dependence of the coefficients on λ and σ is rather indirect. It is easier to determine λ_t, σ_t by the first occurrence of a nonconvex shape of V_{eff} in the symmetric phase, coming from the second-order transition region. The highest order, which is so far available for the six-point susceptibility χ_6^{1PI}, entering the Φ^6-coefficient of V_{eff}, is 16. The number of contributing graphs to order 16 is comparable to the number of graphs contributing to the two-point susceptibility to order 20 and the four-point susceptibility to order 18. An inclusion of higher powers in Φ, say Φ^8, Φ^{10}-terms, would further reduce the order in κ which is tractable. Thus we refrain from further extrapolations, but give bounds on σ_t, derived from $V_{\text{eff}}(\Phi)$ to $O(\kappa^{16})$. They are

$$9.75 \leqslant \sigma_t \leqslant 10.0 \tag{47}$$

The resolution in V_{eff}, within which no nonconvex shape was seen up to $\sigma = 9.75$, was 10^{-7}. Compared to the more reliable result of Eq. (46), the evaluation of V_{eff} seems to lead to an upper bound on σ_t, given by Eq. (47).

5. SUMMARY AND OUTLOOK

In this paper we have generalized hopping parameter expansions from an infinite to a finite volume. The combination of performing the expansions

in a finite volume and to a high (20th) order in the expansion parameter has turned out as a useful computational technique to approach the critical region from the symmetric phase and, in addition, to characterize the type of transition. First- and second-order transitions have been distinguished by various criteria: the monotony criterion referring to the L dependence of response functions (here illustrated on order parameter susceptibilities), the scaling and monotony of the radius of convergence $\kappa_c(L)$ as function of the linear lattice size L, and the effective potential as function of L. In particular, it is the different L dependence of the order parameter susceptibility for first- and second-order transitions in the scaling region (close to but not at the transition point) which allows us to localize tricritical points. The monotony criterion can be applied to Monte Carlo simulations as well; the involved two volumes should be sufficiently large, but both may be finite.

We have applied these methods to renormalizable $O(N)$ models in three dimensions. The plateau structure in the critical exponent $\nu\eta$ in the infinite volume has revealed two universality classes belonging to an $O(N)$-Heisenberg model and to a Gaussian model. Apart from the "trivial" Gaussian behavior at vanishing four- and six-point couplings, we get Gaussian exponents along a tricritical line separating first-and second-order domains. The existence of the first-order domain and the tricritical line is based on the presence of the Φ^6 self-interaction. The $O(N)$ symmetry alone does not determine the critical behavior.

Several extensions are at hand. The first one is from three dimensions to field theories in four dimensions at finite temperature. For a $\Phi^4+\Phi^6$-type theory in four dimensions at finite temperature we expect qualitatively the same infrared behavior and phase structure as for three dimensions, but different values for the critical couplings. A check of the supposed dimensional reduction from four to three dimensions is of particular interest in connection with the electroweak phase transition. Φ^6 terms in the dimensionally reduced $SU(2)$-Higgs model are usually argued to be irrelevant even at the transition to the spontaneously broken phase, and hence dropped.[29] In our extension of the previous investigations we will keep the Φ^6 term in a 4D effective scalar theory at finite temperature, which is derived from the underlying $SU(2)$-Higgs model by integrating out the gauge field degrees of freedom. The phase structure of the effective scalar theory will then be studied in a finite and infinite volume. Hopping parameter expansions are supposed to work the better the smaller is κ, thus the larger are the Higgs masses. Hence this investigation complements the range of Higgs masses which has been available in recent Monte Carlo simulations.[30] One of our aims is to find the *critical* Higgs mass above which the electroweak phase transition ceases to exist. (In case the *physical*

Higgs mass lies above the critical Higgs mass, it is bad news for an explanation of the observed baryon number asymmetry in the universe. The necessary ingredient for an out-of-equilibrium situation can no longer be provided by the electroweak transition if the "transition" turns out to be truly a smooth crossover phenomenon.)

A further application of our computational tools are (tri)critical phenomena in statistical physics. The order of the transition in a superconductor of type II has been recently under debate (refs. 31 and 32 and references therein). The existence of a tricritical point for a suitable Ginzburg–Landau parameter has been conjectured,[33] but a proof of its existence is still outstanding. Work in these directions is in progress.

APPENDIX A. LARGE-COUPLING LIMIT OF $O(N)$ LATTICE MODELS

For $N \geqslant 1$, on a D-dimensional hypercubic lattice Λ, we consider the partition function

$$Z = \int \mathscr{D}\Phi \exp[-S(\Phi)]$$

with corresponding expectation values

$$\langle P \rangle_{\lambda,\sigma} = \frac{1}{Z} \int \mathscr{D}\Phi \, P(\Phi) \exp[-S(\Phi)] \tag{A1}$$

where

$$\mathscr{D}\Phi = \prod_{x \in \Lambda} d^N \Phi_x$$

and

$$S(\Phi) = -\tfrac{1}{2} \sum_{x \neq y} v_{xy} \Phi_x \cdot \Phi_y + \sum_x \mathring{S}(\Phi_x)$$

$$\mathring{S}(\Phi) = \Phi^2 + \lambda(\Phi^2 - 1)^2 + \sigma(\Phi^2 - 1)^3$$

Measure and action are globally $O(N)$-invariant. The observable P should be appropriately bounded so that the integrals exist. Fields at different lattice sites x and y interact by the hopping coupling v_{xy}, which is assumed to obey the following conditions:

$$\begin{gathered} v_{xy} = v_{yx} = v(x-y) \\ v(0) = 0 \\ \sum_{y \in \Lambda} v_{xy} < \infty \\ \sum_{x,\, y \in \Lambda} v_{xy} (\Phi_x - \Phi_y)^2 \geqslant 0 \end{gathered} \tag{A2}$$

As an example, these conditions are satisfied for the pure nearest neighbor interaction, where

$$v_{xy} = 2\kappa \sum_{\mu=0}^{D-1} (\delta_{x,\, y+\hat{\mu}} + \delta_{x,\, y-\hat{\mu}}) \tag{A3}$$

with $\hat{\mu}$ denoting the unit vector in the μ direction. We consider (A1) in the limit $\sigma \to \infty$ with $\lambda = \alpha\sigma$ and α a fixed real number, i.e.,

$$\langle P \rangle_\alpha = \lim_{\sigma \to \infty} \langle P \rangle_{\alpha\sigma,\, \sigma}$$

for

$$\mathring{S}(\Phi) = \Phi^2 + \sigma(\Phi^2 - 1)^2 (\Phi^2 - 1 + \alpha) \tag{A4}$$

The hopping parameters v_{xy} are considered as fixed. We have to select all field configurations that minimize the action in this limit. It is convenient to parametrize the fields according to

$$\Phi_x = u_x v_x, \qquad u_x \in S_{N-1} \qquad \text{(the } N-1 \text{ sphere)}, \qquad v_x \geqslant 0$$

Lemma A.1. As $\sigma \to \infty$ we get the following behavior of expectation values P as dependent on α:

For $\alpha > 1$

$$\langle P \rangle_\alpha = \mathcal{N}_\alpha \prod_{x \in \Lambda} \left(\int_{S_{N-1}} d\Omega_{N-1}(u_x) \right) P(u) \exp[-\tilde{S}(u)]$$

$$\tilde{S}(u) = -\tfrac{1}{2} \sum_{x,\, y \in \Lambda} v_{xy} u_x \cdot u_y$$

For $\alpha = 1$

$$\langle P \rangle_1 = \mathcal{N}_1 \prod_{x \in \Lambda} \left(\sum_{v_x = 0, 1} \left[\int_{S_{N-1}} d\Omega_{N-1}(u_x)\, \delta_{v_x, 1} + \delta_{v_x, 0} \right] \right) \times P(uv) \exp[-\tilde{S}(u, v)]$$

$$\tilde{S}(u, v) = \sum_{x \in \Lambda} v_x^2 - \tfrac{1}{2} \sum_{x, y \in \Lambda} v_{xy} v_x v_y u_x \cdot u_y$$

For $-3 < \alpha < 1$

$$\langle P \rangle_\alpha = P(0)$$

For $\alpha = -3$

$$\langle P \rangle_{-3} = \mathcal{N}_{-3} \prod_{x \in \Lambda} \left(\sum_{v_x = 0, 1} \left[\int_{S_{N-1}} d\Omega_{N-1}(u_x)\, \delta_{v_x, 1} + \delta_{v_x, 0} \right] \right) \times P(\sqrt{3}\, uv) \exp[-\tilde{S}(u, v)]$$

$$\tilde{S}(u, v) = \sum_{x \in \Lambda} 3v_x^2 - \tfrac{3}{2} \sum_{x, y \in \Lambda} v_{xy} v_x v_y u_x \cdot u_y$$

For $\alpha < -3$

$$\langle P \rangle_\alpha = \mathcal{N}_\alpha \prod_{x \in \Lambda} \left(\int_{S_{N-1}} d\Omega_{N-1}(u_x) \right) P\left(\left(1 - \frac{2\alpha}{3} \right) u \right) \exp[-\tilde{S}(u)]$$

$$\tilde{S}(u) = -\frac{1}{2} \sum_{x, y \in \Lambda} \left(1 - \frac{2\alpha}{3} \right) v_{xy} u_x \cdot u_y$$

The $\mathcal{N}_\alpha$ are positive normalization factors independent of P such that $\langle 1 \rangle_\alpha = 1$; $d\Omega_{N-1}$ is the standard measure on the sphere.

For $\alpha > 1$ and $\alpha < -3$ we obtain the $O(N)$ Heisenberg model (Ising model for $N = 1$). For $-3 < \alpha < 1$ the lattice model becomes completely decoupled. At the boundary points $\alpha = 1$ and $\alpha = -3$ the results are "diluted" $O(N)$ models, i.e., $O(N)$ models with additional occupation number variables $v_x \in \{0, 1\}$.

Outline of the Proof. The properties (A2) ensure that the minimizing field configurations of the action $S(\Phi)$ are translation-invariant. Thus it is sufficient to determine the minima of

$$F(\Phi) = (\Phi^2 - 1)^2 (\Phi^2 - 1 + \alpha), \qquad \Phi \in \mathbf{R}^N$$

for the various values of α. Finally the saddle-point expansion for the different cases yields the lemma.

An alternative way to study the large-coupling limit is to perform it termwise in the HPE series of correlation functions. We specialize to the nearest neighbor interaction (A3). The only way the coupling constants λ and σ enter the linked cluster expansion is via the connected one-point vertex couplings $\mathring{v}^c_{2n}(\lambda, \sigma)$, defined in Eq. (11). The connected one-point vertex couplings are related to the full one-point couplings $\mathring{v}_{2n}$ defined by

$$\mathring{v}_{2n} = \frac{\int d^N\Phi\, \Phi_1^{2n} \exp(-\mathring{S}(\Phi))}{\int d^N\Phi \exp(-\mathring{S}(\Phi))} \tag{A5}$$

by the identity (12). At any finite order l, the coefficient of κ^l is a polynomial in the $\mathring{v}^c_{2n}$, hence in the $\mathring{v}_{2n}$. Invoking a saddle-point expansion again, we obtain the following result.

Lemma A.2. Let $\lambda = \alpha\sigma$ with $\sigma > 0$, $-\infty < \alpha < \infty$. Define for non-negative integers N, k

$$\mathscr{A}_{N,k} = (2k-1)!! \frac{\Gamma(N/2)}{\Gamma(N/2+k)\, 2^k}$$

As $\sigma \to \infty$ we get the following results for every $k > 0$:

For $\alpha > 1$

$$\mathring{v}_{2k} = \mathscr{A}_{N,k} + O(\sigma^{-1/2})$$

For $\alpha = 1$

$$\mathring{v}_{2k} = \mathscr{A}_{N,k} \cdot \begin{cases} \dfrac{1}{e+1} + O(\sigma^{-1/2}) & \text{for } N = 1 \\ 1 + O(\sigma^{-1/2}) & \text{for } N \geqslant 2 \end{cases}$$

For $-3 < \alpha < 1$

$$\mathring{v}_{2k} = \frac{(2k-1)!!}{2^k} \frac{1}{[(3-2\alpha)\,\sigma]^k} [1 + O(\sigma^{-1/2})]$$

For $\alpha = -3$

$$\mathring{v}_{2k} = \mathscr{A}_{N,k} \cdot \begin{cases} \dfrac{3^k}{e^3+1} + O(\sigma^{-1/2}) & \text{for } N = 1 \\ 3^k + O(\sigma^{-1/2}) & \text{for } N \geqslant 2 \end{cases}$$

For $\alpha < -3$

$$\mathring{v}_{2k} = \mathscr{A}_{N,k}\left(1 - \frac{2\alpha}{3}\right)^k + O(\sigma^{-1/2})$$

For $\alpha > 1$ the vertices are identical with those of the $O(N)$ Heisenberg models. In the range $-3 < \alpha < 1$ they agree with the vertices of a purely Gaussian model with ultralocal action

$$\mathring{S}(\Phi) = (3 - 2\alpha)\,\sigma\Phi^2$$

leading to complete disorder as $\sigma \to \infty$ for every finite κ. For $\alpha < -3$ we obtain the Heisenberg model again, as can be seen as follows. For any $\beta > 0$, rescaling of the vertices

$$\mathring{v}_{2k} \to \beta^{2k}\mathring{v}_{2k} \tag{A6}$$

implies a corresponding rescaling of the connected vertices, $\mathring{v}^c_{2k} \to \beta^{2k}\mathring{v}^c_{2k}$; cf. (12). In turn, elementary graph theory shows that all susceptibilities change according to $\chi_n(\kappa) \to \beta^n \chi_n(\beta^2\kappa)$. Hence, universality classes are invariant under (A6). Furthermore, we see that, for $N \geqslant 2$, the boundary points $\alpha = 1$ and $\alpha = -3$ belong to the Heisenberg class as well. A remnant of the occupation number variables is only seen in the case of $N = 1$, which is a remarkable exception and needs further study.

Thermodynamic quantities like χ and the critical coupling κ_c can be directly determined in these limiting models. Alternatively, one may start with the original action (A4) at finite σ, calculate χ and κ_c in the HPE, and take the large-coupling limit last. Our results indicate that both limits commute.

APPENDIX B. EXAMPLE OF SERIES EXPANSIONS FOR THE TWO-POINT SUSCEPTIBILITY

In Tables IV and V we list the expansion coefficients of the two-point susceptibility χ_2 of (5), written as

$$\chi_{2n}(\kappa, \lambda, \sigma; L) = \sum_{\mu \geqslant 0} b_\mu(\lambda, \sigma; L)(2\kappa)^\mu \tag{B1}$$

for $\mu = 0, \ldots, 20$ for the three-dimensional $O(4)$ model for two pairs of four- and six-point couplings (λ, σ) and various volumes L^3. The values of the coupling constants are chosen somewhat above and below the tricritical

Table IV. Series Coefficients of the Two-Point Susceptibility χ_2 as Defined in (54) for Various Lattice Volumes L^3, for the $O(4)$ Model (1)–(2), at Coupling Constants $\sigma = 5.0$ and $\lambda = \sigma/2 = 2.5$[a]

	$L=4$	$L=6$	$L=8$	$L=\infty$
b_0	1.767811187e−01	1.767811187e−01	1.767811187e−01	1.767811187e−01
b_1	1.875093835e−01	1.875093835e−01	1.875093835e−01	1.875093835e−01
b_2	1.900125602e−01	1.900125602e−01	1.900125602e−01	1.900125602e−01
b_3	1.922690391e−01	1.922690391e−01	1.922690391e−01	1.922690391e−01
b_4	1.892950458e−01	1.895724394e−01	1.895724394e−01	1.895724394e−01
b_5	1.859873544e−01	1.865626788e−01	1.865626788e−01	1.865626788e−01
b_6	1.798987466e−01	1.813634027e−01	1.813720717e−01	1.813720717e−01
b_7	1.736631729e−01	1.760492597e−01	1.760672395e−01	1.760672395e−01
b_8	1.655675951e−01	1.696450984e−01	1.697046433e−01	1.697049142e−01
b_9	1.574955741e−01	1.632781592e−01	1.633812919e−01	1.633818538e−01
b_{10}	1.480384104e−01	1.56347487e−01	1.565621324e−01	1.565645676e−01
b_{11}	1.387554403e−01	1.49555404e−01	1.498846763e−01	1.498890906e−01
b_{12}	1.284275569e−01	1.42474718e−01	1.430203492e−01	1.430317221e−01
b_{13}	1.184138401e−01	1.35597992e−01	1.363618800e−01	1.363804958e−01
b_{14}	1.076646157e−01	1.28586645e−01	1.296905927e−01	1.297270665e−01
b_{15}	9.736049025e−02	1.21820599e−01	1.232616678e−01	1.233164494e−01
b_{16}	8.662646939e−02	1.15013182e−01	1.169170337e−01	1.170075094e−01
b_{17}	7.645556689e−02	1.08476663e−01	1.108321311e−01	1.109586639e−01
b_{18}	6.615059713e−02	1.01960177e−01	1.048837366e−01	1.050700011e−01
b_{19}	5.650721931e−02	9.57296188e−02	9.919968582e−02	9.944545683e−02
b_{20}	4.696691839e−02	8.95442302e−02	9.366035412e−02	9.399383161e−02

[a] These couplings belong to the second-order transition region.

point along the line $\lambda = \sigma/2$ in bare coupling space. At $\lambda = 2.5$ the model has a second-order transition, whereas at $\lambda = 5.0$ the transition is of first order.

For every μ, the coefficient $b_\mu(\lambda, \sigma; L)$ is a polynomial in the coupling $\hat{v}_{2n}(\lambda, \sigma)$'s defined in (13). Hence it is a real number. Questions of convergence, conditioning, etc. of the series are the same as in the case of a lattice unbounded in all directions. A convenient way to avoid severe roundoff errors is to combine graphs into further equivalence classes, so-called vertex structures.[8] They are considerably less in number and smaller in size than the objects related to graphs. Therefore the errors induced by alternating signs of the $\hat{v}_{2n}(\lambda, \sigma)^c$ and the roundoff errors of the attached rational weight factors do not accumulate beyond the numerical precision to which the integrals (13) are evaluated. The integration has been performed up to 12 digits. Thus the coefficents b_μ of the tables are given within 10 digits.

Table V. As in Table IV, but at Coupling Constants $\sigma = 10.0$ and $\lambda = \sigma/2 = 5.0$[a]

	$L=4$	$L=6$	$L=8$	$L=\infty$
b_0	1.023127641e−01	1.023127641e−01	1.023127641e−01	1.023127641e−01
b_1	6.280741021e−02	6.280741021e−02	6.280741021e−02	6.280741021e−02
b_2	4.448843062e−02	4.448843062e−02	4.448843062e−02	4.448843062e−02
b_3	3.113896834e−02	3.113896834e−02	3.113896834e−02	3.113896834e−02
b_4	2.196504376e−02	2.190294365e−02	2.190294365e−02	2.190294365e−02
b_5	1.544217140e−02	1.536006216e−02	1.536006216e−02	1.536006216e−02
b_6	1.088285598e−02	1.076585896e−02	1.076520890e−02	1.076520890e−02
b_7	7.657062683e−03	7.537225091e−03	7.536365580e−03	7.536365580e−03
b_8	5.398747329e−03	5.272544257e−03	5.270872836e−03	5.270866032e−03
b_9	3.802721557e−03	3.686832508e−03	3.684987419e−03	3.684978422e−03
b_{10}	2.683949486e−03	2.576214776e−03	2.573803375e−03	2.573779992e−03
b_{11}	1.892949088e−03	1.799916511e−03	1.797512184e−03	1.797485086e−03
b_{12}	1.337653766e−03	1.256926602e−03	1.254314388e−03	1.254270283e−03
b_{13}	9.446796670e−04	8.777073102e−04	8.752769968e−04	8.752301854e−04
b_{14}	6.683322686e−04	6.127194998e−04	6.103503216e−04	6.102899361e−04
b_{15}	4.725723889e−04	4.277289504e−04	4.256333206e−04	4.255733755e−04
b_{16}	3.346632114e−04	2.985492698e−04	2.966459680e−04	2.965788682e−04
b_{17}	2.368883466e−04	2.083823901e−04	2.067618926e−04	2.066986937e−04
b_{18}	1.678883648e−04	1.454448101e−04	1.440438674e−04	1.439795485e−04
b_{19}	1.189384952e−04	1.015154745e−04	1.003574216e−04	1.002993328e−04
b_{20}	8.435105473e−05	7.086546783e−05	6.989953824e−05	6.984428669e−05

[a] These coupling constants belong to the first-order transition region.

To compute the coefficents b_μ for other choices of couplings, it is not necessary to recalculate the contributions of all single graphs, but just the $\mathring{v}_{2n}(\lambda, \sigma)^c$, once the vertex structures are given. For details we refer to ref. 8.

ACKNOWLEDGMENT

T.R. is a Heisenberg Fellow.

REFERENCES

1. H. Meyer-Ortmanns, Phase transitions in quantum chromodynamics, *Rev. Mod. Phys.* **68**:473 (1996).
2. M. Wortis, Linked cluster expansion, in *Phase Transition and Critical Phenomena*, Vol. 3, C. Domb and M. S. Green, eds. (Academic Press, London, 1974).
3. C. Itzykson and J.-M. Drouffe, *Statistical Field Theory*, Vol. 2 (Cambridge University Press, Cambridge, 1989).
4. A. J. Guttmann, Asymptotic analysis of power-series expansions, in *Phase Transitions and Critical Phenomena*, Vol. 13, C. Domb and J. L. Lebowitz, eds. (Academic Press, London, 1989).

5. M. Lüscher and P. Weisz, *Nucl. Phys. B* **300**[FS22]:325 (1988).
6. M. Lüscher and P. Weisz, *Nucl. Phys. B* **290**[FS20]:25 (1987).
7. M. Lüscher and P. Weisz, *Nucl. Phys. B* **295**[FS21]:65 (1988).
8. T. Reisz, *Nucl. Phys. B* **450**:569 (1995).
9. T. Reisz, *Phys. Lett. B* **360**:77 (1995).
10. F. Wilczek, *Int. J. Mod. Phys. A* **7**:3911 (1992).
11. K. Rajagopal and F. Wilczek, *Nucl. Phys. B* **399**:395, **404**:577 (1993).
12. A. Pordt, A convergence proof for linked cluster expansions, MS-TPI-96-05 [hep-lat 9604010].
13. A. Pordt and T. Reisz, Linked cluster expansions beyond nearest neighbour interactions: Convergence and graph classes, HD-THEP-96-09, MS-TPI-96-06 [hep-lat 9604021] to appear in *Int. J. Mod. Phys. A*.
14. H. Meyer-Ortmanns and F. Karsch, *Phys. Lett.* **193B**:489 (1987).
15. P. Butera and M. Comi, New extended high temperature series for the N-vector spin models on three-dimensional bipartite lattices [hep-lat 9505027].
16. M. Campostrini, A. Pelissetto, P. Rossi, and E. Vicari, Strong coupling expansion of lattice $O(N)$ sigma models [hep-lat 9509025].
17. M. N. Barbour, In *Phase Transitions and Critical Phenomena*, Vol. 8, C. Domb and J. L. Lebowitz, eds. (Academic Press, New York, 1983), p. 145.
18. K. Binder and D. P. Landau, *Phys. Rev. B* **30**:1477 (1984); K. Binder, *Rep. Prog. Phys.* **50**:783 (1987).
19. C. Borgs and J. Z. Imbrie, *Commun. Math. Phys.* **123**:305 (1989); C. Borgs and R. Kotecky, *J. Stat. Phys.* **61**:79 (1990); C. Borgs and R. Kotecky, *Phys. Rev. Lett.* **68**:1734 (1992).
20. C. Borgs, R. Kotecky, and S. Miracle-Sole, *J. Stat. Phys.* **62**:529 (1991).
21. D. S. Gaunt and A. J. Guttmann, Asymptotic analysis of coefficients, in *Phase Transition and Critical Phenomena*, Vol. 3, C. Domb and M. S. Green, eds. (Academic Press, London, 1974).
22. M. Blume, *Phys. Rev.* **141**:517 (1966).
23. H. W. Capel, *Physica* **32**:966 (1966).
24. M. Blume, V. J. Emery, and R. B. Griffiths, *Phys. Rev. A* **4**:1071 (1971).
25. J. Glimm and A. Jaffe, *Quantum Physics, A Functional Point of View*, 2nd ed. (Springer, Berlin, 1987).
26. R. Fernandez, J. Fröhlich, and A. D. Sokal, *Random Walks, Critical Phenomena, and Triviality in Quantum Field Theory* (Springer-Verlag, Berlin, 1992).
27. G. A. Baker, Jr., and J. D. Johnson, *J. Math. Phys.* **28**:1146 (1987).
28. T. Hara, T. Hattori, and H. Tasaki, *J. Math. Phys.* **26**:2922 (1985).
29. K. Kajantie, M. Laine, K. Remmukainen, and M. Shaposhnikov, *Nucl. Phys. B* **458**:90 (1996).
30. Z. Fodor, J. Hein, K. Jansen, A. Jaster, and I. Montvay, *Nucl. Phys. B* **439**:147 (1995).
31. L. Radzikovsky, *Europhys. Lett.* **29**:227 (1995).
32. B. Bergerhoff, F. Freire, D. Litim, S. Lola, and C. Wetterich, *Phys. Rev. B* **53**:5734 (1996).
33. J. Bartholomew, *Phys. Rev. B* **28**:5378 (1983).
34. A. Esser, V. Dohm, and X. S. Chen, *Physica A* **222**:355 (1995).